# ChemInform Abstract: Structure, Stability, and Cluster-Cage Interactions in Nitride Clusterfullerenes M3N@C2n (M: Sc, Y; 2n = 68—98): A Density Functional Theory Study

**ARTICLE** *in* JOURNAL OF THE AMERICAN CHEMICAL SOCIETY · OCTOBER 2007

Impact Factor: 12.11 · DOI: 10.1021/ja073809l · Source: PubMed



**2 AUTHORS**, INCLUDING:

Alexey A Popov

Leibniz Institute for Solid State and Materials…

**188** PUBLICATIONS **3,410** CITATIONS

SEE PROFILE

# Structure, stability and cluster-cage interactions in nitride clusterfullerenes $M_3N@C_{2n}$ (M = Sc, Y; $2n$ = 68 – 98): a density functional theory study

*Alexey A. Popov,*[*,†] and Lothar Dunsch*[‡]

Chemistry Department, Moscow State University, Moscow 119992, Russia,

Group of Electrochemistry and Conducting Polymers, Leibniz-Institute for Solid State and Materials Research Dresden, D-01171 Dresden, Germany

AUTHOR EMAIL ADDRESS: popov@phys.chem.msu.ru

**RECEIVED DATE (to be automatically inserted after your manuscript is accepted if required according to the journal that you are submitting your paper to)**

* To whom correspondence should be addressed. E-mail: popov@phys.chem.msu.ru (A.A.P.)

† Moscow State University

‡ Leibniz-Institute for Solid State and Materials Research Dresden

**ABSTRACT**. Extensive semiempirical calculations of the hexaanions of IPR (isolated pentagon rule) and non-IPR isomers of $C_{68}$–$C_{88}$ and IPR isomers of $C_{90}$–$C_{98}$ followed by DFT calculations of the lowest energy structures were performed to find the carbon cages that can provide the most stable isomers of $M_3N@C_{2n}$ clusterfullerenes (M = Sc, Y) with Y as a model for rare earth ions. DFT calculations of isomers of $M_3N@C_{2n}$ (M = Sc, Y; $2n$ = 68 – 98) based on the most stable $C_{2n}^{6-}$ cages were also performed. The lowest energy isomers found by this methodology for $Sc_3N@C_{68}$, $Sc_3N@C_{78}$, $Sc_3N@C_{80}$, $Y_3N@C_{78}$, $Y_3N@C_{80}$, $Y_3N@C_{84}$, $Y_3N@C_{86}$, and $Y_3N@C_{88}$ are those that have been shown to exist by single-crystal X-ray studies as $Sc_3N@C_{2n}$ ($2n$ = 68, 78, 80), $Dy_3N@C_{80}$, and $Tb_3N@C_{2n}$ ($2n$ = 80, 84, 86, 88) clusterfullerenes. Reassignment of the carbon cage of $Sc_2@C_{76}$ to the non-IPR $C_s$: 17490 isomer is also proposed. The stability of nitride clusterfullerenes was found to correlate well with the stability of the empty 6-fold charged cages. However, the dimensions of the cage in terms of its ability to encapsulate $M_3N$ clusters were also found to be an important factor, especially for the medium size cages and the large $Y_3N$ cluster. In some cases the most stable structures are based on the different cage isomers for $Sc_3N$ and $Y_3N$ clusters. Up to the cage size of $C_{84}$, non-IPR isomers of $C_{2n}^{6-}$ and $M_3N@C_{2n}$ were found to compete with or to be even more stable than IPR isomers. However, the number of adjacent pentagon pairs in the most stable non-IPR isomers decreases as cage size increases: the most stable $M_3N@C_{2n}$ isomers have three such pairs for $2n$ = 68 – 72, two pairs for $n$ = 74 – 80, and only one pair for $n$ = 82, 84. For $C_{86}$ and $C_{88}$ the lowest energy IPR isomers are much more stable than any non-IPR isomer. The trends in the stability of the fullerene isomers and the cluster-cage binding energies are discussed and general rules for stability of clusterfullerenes are established. Finally, the high yield of $M_3N@C_{80}$ ($I_h$) clusterfullerenes for any metal is explained by the exceptional stability of $C_{80}^{6-}$ ($I_h$: 31924) cage, rationalized by the optimum distribution of the pentagons leading to the minimization of the steric strain, and structural similarities of $C_{80}$ ($I_h$: 31924) with the lowest energy non-IPR isomers of $C_{76}^{6-}$, $C_{78}^{6-}$, $C_{82}^{6-}$, and $C_{84}^{6-}$ are pointed out.

**KEYWORDS:** endohedral fullerenes, nitride clusterfullerenes, DFT calculations, isolated-pentagon rule, molecular structure.

## Introduction

The world of endohedral fullerenes has been largely expanded in the last decade by the introduction of nitride clusterfullerenes with a variety of carbon cages and encaged clusters.[1-3] Historically, the first member of nitride clusterfullerenes was $Sc_3N@C_{80}$ ($I_h$: 31924), isolated and structurally characterized by Stevenson et al.[4] in 1999. It remains the most abundant structure of this clusterfullerene family up till now. The class of $Sc_3N$-based clusterfullerenes also includes $D_3$-$Sc_3N@C_{68}$,[5, 6] $D_{3h}$-$Sc_3N@C_{78}$,[7] the isomer of $Sc_3N@C_{80}$ with $D_{5h}$-symmetric carbon cage,[8-10] and the recently reported compound $Sc_3N@C_{70}$.[11] Significantly, $Sc_3N@C_{68}$ and $Sc_3N@C_{70}$ are based on fullerene isomers that do not obey the isolated pentagon rule (IPR). Substantial efforts by several groups to synthesize different nitride clusterfullerenes resulted in the isolation of $M_3N@C_{80}$ (M = Y and all lanthanides from Gd to Lu),[12-17] a series of mixed $Er_xSc_{3-x}N@C_{68}$ ($x$ = 1, 2)[5] and $M_xSc_{3-x}N@C_{80}$ clusterfullerenes (M = Er[4, 12] or Gd,[18] $x$ = 1, 2; M = Ce, $x$ = 1[19]), and even $ScYErN@C_{80}$,[20] a clusterfullerene with three different metals. Development of the reactive gas atmosphere methodology made the isolation of a larger variety of cluster fullerenes possible, including the families $Gd_3N@C_{2n}$ ($2n$ = 80 – 88),[16] $Tm_3N@C_{2n}$ ($2n$ = 78–88),[13] $Dy_3N@C_{2n}$ ($2n$ = 76–98).[21] In addition, the isolation of $Tb_3N@C_{2n}$ ($2n$ = 80, 84 – 88) clusterfullerenes was recently reported.[22, 23]

Unambiguous structural characterization of clusterfullerenes, at least in terms of the cage isomer present, can be provided by single-crystal X-ray diffraction in some cases. Clusterfullerenes based on the $C_{80}$ ($I_h$: 31924) cage isomer remain the most studied ones: single-crystal X-ray structures were reported for $Sc_3N@C_{80}$,[4] $Lu_3N@C_{80}$,[24] $Dy_3N@C_{80}$,[25] $Tb_3N@C_{80}$,[23] $ErSc_2N@C_{80}$,[26] and $CeSc_2N@C_{80}$.[19] Crystallographic reports on other clusterfullerenes include two studies with the $C_{80}$ ($D_{5h}$: 31923) cage, $Sc_3N@C_{80}$[10] and $Tb_3N@C_{80}$,[23] as well as reports on $Sc_3N@C_{68}$,[6] $Sc_3N@C_{78}$,[7] $Tb_3N@C_{84}$,[22] $Tb_3N@C_{86}$,[23] and $Tb_3N@C_{88}$.[23] The cage isomers found for $Tb_3N@C_{2n}$ can be assigned to the Gd-, Dy-, and Tm-based clusterfullerenes because their UV-Vis spectra are very similar. However, the structures of the clusterfullerenes with other cages ($2n$ = 76, 82, 90–98) remain unknown. The available amounts are simply too small to grow diffraction-quality single crystals. $^{13}C$ NMR spectroscopy also requires

considerable amounts of the endohedral fullerenes; besides, it provides only the cage symmetry, and hence this information may be ambiguous, especially if it is taken into account that non-IPR isomers may be formed, as documented in recent works.[6, 11, 23, 27-30] Theoretical studies can aid in the structural determination, or at least can narrow down the possible list of isomeric structures to consider them in spectroscopic studies. The early theoretical studies focused on the possible isomerism of endohedral fullerenes,[31, 32] and though they were limited to only IPR isomers, an important feature of the endohedral fullerenes was revealed – experimentally isolated isomers of empty and endohedral fullerenes are usually different because encapsulated metals or clusters transfer some of their electrons to the carbon cage, and relative stabilities of the fullerene isomers may alter for different charge states.

The electronic structure of nitride clusterfullerenes may be conceived as a result of a 6-fold electron transfer from the cluster to the fullerene. Though the $M_3N^{6+}@C_{2n}^{6-}$ ionic model was questioned in recent studies and much smaller net charges of the cluster and the cage as well as strong covalent cluster-cage interactions were established,[33-37] the ionic model is still useful for developing stability criteria of nitride clusterfullerenes. The simplest and elegant use of this conjecture to predict the most suitable cage isomers capable of encapsulating nitride cluster was proposed by Campanera et al.[38] Assuming the 6-fold electron transfer in nitride clusterfullerenes, the authors have supposed that only the fullerenes with a considerable gap between LUMO+2 and LUMO+3 (which become HOMO and LUMO, respectively, in the $C_{2n}^{6-}$ hexaanion and presumably in $M_3N@C_{2n}$) may be considered as a suitable hosts for nitride clusters. Screening all IPR fullerenes in the $C_{60}$ – $C_{84}$ range, they have found that only $C_{60}$, $C_{78}$ ($D_{3h}$: 24109), and $C_{80}$ ($I_h$: 31924 and $D_{5h}$: 31923) may be considered as a suitable cage isomers. Indeed, besides $C_{60}$, which appears to be too small to host a $Sc_3N$ cluster, only these and no other IPR cage isomers were found among $Sc_3N@C_{2n}$ clusterfullerenes. However, the growing number of non-IPR isomers reported to date, including nitride clusterfullerenes $Sc_3N@C_{68}$,[5] $Sc_3N@C_{70}$,[11] $Tb_3N@C_{84}$,[22] and $M_3N@C_{78}$ (M = Dy, Tm),[39] demonstrates that IPR cannot be considered as a firm limitation for the stability of an endohedral fullerene. Thus, a consideration of hundreds and thousands of isomers is required, and therefore the method proposed by Campanera et al.[38] cannot be used to

distinguish the most suitable cages because many isomers with suitable gaps may be found among those thousands of possible cage isoemrs. In fact, the argument of the necessity of the large HOMO-LUMO gap is essential for kinetic stability, but it cannot discriminate the isomers with different thermodynamic stability.

It is reasonable to conceive that the stability of the cage isomers of endohedral fullerenes should correlate with the stability of the appropriately charged empty cages, the charge being the function of the metal or the cluster composition incorporated.[1, 28, 31, 33] Thus, we have suggested that the stability of the clusterfullerene isomers should correlate with the stability of the fullerene cages in the hexaanionic state. Screening through the large number of IPR and non-IPR isomers of $C_{70}$ and $C_{78}$ with subsequent DFT calculations, we have proposed the molecular structures of $Sc_3N@C_{70}$[11] and $M_3N@C_{78}$ (M = Dy, Tm),[39] which both were found to be non-IPR fullerenes, and confirmed these findings by the comparison of experimental and DFT predicted spectroscopic data. The study of $M_3N@C_{78}$ also revealed that the cluster size has a strong effect on the carbon cage isomerism, as the IPR isomer $D_{3h}$: 24109 is more stable for the relatively small $Sc_3N$ cluster in $Sc_3N@C_{78}$, while the lowest energy isomer with $Y_3N$ and the clusters of similar size is based on the non-IPR $C_2$: 22010 cage.[39] In this work, we apply this methodology for the whole range of carbon cages observed for $M_3N@C_{2n}$ so far (e.g., $C_{68}$ – $C_{98}$) to predict the most possible structures of $M_3N@C_{76}$ – $M_3N@C_{98}$ (M = Dy, Tm, Tb). Some of them were isolated but not yet structurally characterized, while others were observed in the mass spectra of the clusterfullerene extracts only, but not yet isolated. The data obtained thus for a broad range of cage sizes enabled us to establish general trends in stability of nitride clusterfullerenes.

**Computational details**

Semiempirical calculations at the AM1[40] level were performed using PC GAMESS package.[41] DFT calculations were performed using PBE functional[42] and TZ2P-quality basis set with SBK-type effective core potential for Sc, and Y atoms implemented in the PRIRODA package.[43, 44] The quantum-chemical

code employed expansion of the electron density in an auxiliary basis set to accelerate evaluation of the Coulomb and exchange-correlation terms. No symmetry constrains were adopted in the optimization.

**Results**

Treating the stability criteria of endohedral fullerenes we generally propose that fullerene isomers with three or more fused pentagons cannot be efficiently stabilized by a $M_3N$ cluster and will thus be unstable. Hence, in this work we have considered only IPR isomers or non-IPR isomers with isolated pairs of adjacent pentagons (APPs). The number of such isomers increases from 359 for $C_{68}$ to 16717 for $C_{88}$. For $C_{90}$ – $C_{98}$ only IPR isomers were considered (the reasons the for exclusion of non-IPR isomers are described below). The total amount of isomers of $C_{2n}$ cages studied for each 2*n* and the numbers of the isomers according to spiral algorithm are listed in Table 1. For all these fullerenes, hexaanion structures were optimized at the AM1 level. Then, the most stable isomers (10 to 20 for each cage size) were optimized at the DFT level to ensure the reliability of AM1-predicted relative energies, and finally $Sc_3N@C_{2n}$ and $Y_3N@C_{2n}$ clusterfullerenes based on the most stable $C_{2n}^{6-}$ isomers were studied by DFT. We have recently shown that the ionic radii of the cluster-forming metal largely determine the cluster-cage interactions as well as the spectroscopic properties of clusterfullerenes. Since the ionic radius of Y (0.90 Å) is close to that of Dy (0.91 Å), and only slightly smaller than that of Tb (0.92 Å) and slightly larger than that of Tm (0.87 Å),[45] the structures and spectroscopic properties of $Y_3N@C_{2n}$ isomers and those of $M_3N@C_{2n}$ (M = Tb, Dy, Tm) clusterfullerenes are assumed to be similar.[25, 39] Thus, the calculated relative energies of $Y_3N@C_{2n}$ isomers are to a great extent applicable to the lanthanide-based clusterfullerenes, and we consider Y as a model for rare earth metal ions of similar radii.

Relative energies and HOMO-LUMO gaps of the $C_{2n}^{6-}$ and the corresponding $Sc_3N@C_{2n}$ and $Y_3N@C_{2n}$ isomers are listed in tables 2-4. Whenever the relative energy (denoted also as $\Delta E$) is discussed hereafter either for the empty cages or the clusterfullerenes, it is given versus the energy of the

***Table 1.*** The list of $C_{2n}$ isomers, the hexaanions of which are studied in this work.[a]

| $C_{2n}$ | N[b] | isomer Nos.[c] | N (IPR)[d] | IPR Nos.[e] |
|---|---|---|---|---|
| $C_{68}$ | 359 | 5974 – 6332 | 0 | – |
| $C_{70}$ | 527 | 7629 – 8154 | 1 | $D_{5h}$: 8149 |
| $C_{72}$ | 906 | 10285 – 11190 | 1 | $D_{6d}$: 11190 |
| $C_{74}$ | 1296 | 12951 – 14246 | 1 | $D_{3h}$: 14246 |
| $C_{76}$ | 2056 | 17096 – 19151 | 2 | $D_2$: 19150, $T_d$: 19151 |
| $C_{78}$ | 2927 | 21183 – 24109 | 5 | 24105 – 24109 |
| $C_{80}$ | 4442 | 27483 – 31924 | 7 | 31918 – 31924 |
| $C_{82}$ | 6091 | 33628 – 39718 | 9 | 39710 – 39718 |
| $C_{84}$ | 8831 | 42762 – 51592 | 24 | 51569 – 51592 |
| $C_{86}$ | 11873 | 51890 – 63761 | 19 | 63743 – 63761 |
| $C_{88}$ | 16717 | 65022 – 81738 | 35 | 81704 – 81738 |
| $C_{90}$ | | | 46 | 99873 – 99918 [f] |
| $C_{92}$ | | | 86 | 126324 – 126409 [f] |
| $C_{94}$ | | | 134 | 153360 – 153493 [f] |
| $C_{96}$ | | | 187 | 191653 – 191839 [f] |
| $C_{98}$ | | | 259 | 230759 – 231017 [f] |

[a] The isomers of $C_{70}^{6-}$ and $C_{78}^{6-}$ were studied in Ref. 11 and Ref. 39, respectively

[b, c] total number of isomers studied in the hexaanionic at the AM1 level, and the range of their numbers according to spiral algorithm (Ref. 46)

[d, e] total number of IPR isomers of $C_{2n}$ for a given $2n$, and the range of their numbers according to the spiral algorithm (Ref. 46)

[f] only IPR isomers are studied for $C_{90}$–$C_{98}$, and for these fullerenes we use the truncated numbering system which counts only IPR isomers. That is, isomer $C_{90}$ ($D_{5h}$: 99873) is designated as $C_{90}$ ($D_{5h}$: 1), isomer $C_{90}$ ($C_{2v}$: 99874) as $C_{90}$ ($C_{2v}$: 2), isomer $C_{92}$ ($D_2$: 126324) as $C_{92}$ ($D_2$: 1), etc.

most stable isomer with the same 2*n*. Since $C_{76}$ is the smallest fullerene for which $Dy_3N@C_{2n}$ was found in the cluster fullerene extract,[21] systematic calculations (that is, with consideration of at least ten lowest energy $C_{2n}^{6-}$isomers) for smaller fullerenes were performed only for the $Sc_3N$ cluster, while computations of $Y_3N@C_{2n}$ were limited for these cages to the selected isomers, which had the lowest energies for $Sc_3N@C_{2n}$ or could be considered as relatively stable structures based on the cage shape and size. For $C_{76}$–$C_{88}$, systematic computations were performed both for $Sc_3N$ and $Y_3N$. Selected $Y_3N@C_{2n}$ and $Sc_3N@C_{2n}$ isomers were considered for $C_{90}$ – $C_{98}$, usually limited to one or few most stable $C_{2n}^{6-}$cages with the largest HOMO-LUMO gaps. Whenever $M_3N$ will be used hereafter to designate trimetallic nitride cluster in the description of the results or in the discussion, it is assumed that these results or observations are valid for both $Sc_3N$ and $Y_3N$. The ideal symmetry of the cage and its number according to the Fowler spiral numbering scheme[46] divided by a colon will be used to label carbon cage isomers. With this respect it should be noted that the symmetry of $M_3N@C_{2n}$ is not necessarily the same as the symmetry of the empty fullerene, and in many cases the former appears to be lower. When the $M_3N$ cluster geometry in the optimized $M_3N@C_{2n}$ structures is discussed, the degree of the cluster pyramidalization is represented by *h*, the displacement of the nitrogen atom out of the plane formed by the three metal atoms (that is, *h* is the height of the pyramid formed by the three metal atoms and the N atom in the vertex). In some cases, especially for IPR isomers, several isomers based on the same carbon cage and different in the position of the cluster are possible. In such cases the data listed in tables 2–4 correspond to the most stable structures found by optimization of several possible conformations.

**$M_3N@C_{68}$**. The most stable isomer of $C_{68}^{6-}$ among all studied structures is $D_3$: 6140 with three APPs. It is almost isoenergetic to the isomer $C_{2v}$: 6073, which has two APPs ($\Delta E$ = 8.8 kJ/mol), while other isomers of $C_{68}^{6-}$ are considerably less stable ($\Delta E$ = 47.7 kJ/mol or more). Among the ten most stable isomers, $D_3$: 6140 has the largest HOMO-LUMO gap, 1.20 eV. $D_3$: 6140 is also the most stable isomer of $Sc_3N@C_{68}$ (Fig. 1), however the stability order of other isomers is significantly different from that of

***Table 2.*** Relative energies (Δ*E*, kJ/mol), HOMO-LUMO gaps (gap, eV), and binding energies (BE-2, eV) of the most stable $C_{2n}^{6-}$ and $Sc_3N@C_{2n}$ ($2n$ = 68, 70, 72, 74) isomers as computed at the DFT level

| | Cage | | $C_{2n}^{6-}$ | | $Sc_3N@C_{2n}$ | | | Cage | | $C_{2n}^{6-}$ | | $Sc_3N@C_{2n}$ | |
|---|---|---|---|---|---|---|---|---|---|---|---|---|---|
| $C_{2n}$ | isomer | APPs | Δ*E* | gap | Δ*E* | gap | $C_{2n}$ | isomer | APPs | Δ*E* | gap | Δ*E* | gap |
| $C_{68}$ | $D_3$: 6140 | 3 | 0.0 | 1.20 | 0.0 | 1.28 | $C_{70}$ | $C_{2v}$: 7854 | 3 | 0.0 | 1.24 | 0.0 | 1.29 |
| $C_{68}$ | $C_{2v}$: 6073 | 2 | 8.8 | 0.65 | 246.0 | 0.53 | $C_{70}$ | $C_2$: 7957 | 2 | 17.6 | 0.93 | 140.0 | 0.91 |
| $C_{68}$ | $C_1$: 6102 | 3 | 47.7 | 0.98 | 95.6 | 0.94 | $C_{70}$ | $C_1$: 7852 | 3 | 41.8 | 0.75 | 21.6 | 0.83 |
| $C_{68}$ | $C_2$: 6118 | 3 | 54.5 | 0.71 | 71.4 | 0.77 | $C_{70}$ | $D_{5h}$: 8149 | 0 | 42.9 | 0.50 | 163.7 | 0.53 |
| $C_{68}$ | $C_2$: 6146 | 2 | 62.8 | 0.58 | 191.7 | 0.62 | $C_{70}$ | $C_s$: 7960 | 2 | 48.6 | 0.96 | 179.0 | 1.00 |
| $C_{68}$ | $C_s$: 6072 | 3 | 81.3 | 0.68 | 205.9 | 0.74 | $C_{70}$ | $C_1$: 7886 | 3 | 54.7 | 0.84 | 39.2 | 0.91 |
| $C_{68}$ | $C_s$: 6089 | 3 | 73.6 | 1.08 | 256.9 | 1.01 | $C_{70}$ | $C_s$: 7922 | 3 | 56.1 | 0.94 | 68.0 | 0.85 |
| $C_{68}$ | $C_1$: 6138 | 3 | 70.1 | 1.04 | 87.9 | 1.03 | $C_{70}$ | $C_1$: 7887 | 3 | 56.8 | 0.65 | 43.6 | 0.65 |
| $C_{68}$ | $C_1$: 6116 | 3 | 90.5 | 0.39 | 123.9 | 0.48 | $C_{70}$ | $C_1$: 7851 | 3 | 61.8 | 0.57 | 28.6 | 0.61 |
| $C_{68}$ | $C_1$: 6039 | 3 | 91.0 | 0.45 | 200.9 | 0.53 | $C_{70}$ | $C_1$: 7849 | 3 | 69.4 | 0.90 | 35.6 | 0.88 |
| | | | | | | | | | | | | | |
| $C_{72}$ | $D_2$: 10611 | 2 | 0.0 | 1.12 | 54.6 | 0.89 | $C_{74}$ | $C_2$: 13295 | 2 | 0.0 | 1.22 | 18.7 | 1.04 |
| $C_{72}$ | $C_1$: 10610 | 2 | 68.7 | 0.72 | 34.6 | 0.75 | $C_{74}$ | $C_2$: 13333 | 2 | 23.2 | 0.64 | 51.3 | 0.73 |
| $C_{72}$ | $C_s$: 10616 | 2 | 71.3 | 0.53 | 49.9 | 0.54 | $C_{74}$ | $D_{3h}$: 14246 | 0 | 25.9 | 0.71 | 21.3 | 0.47 |
| $C_{72}$ | $C_1$: 10482 | 3 | 77.0 | 1.01 | 26.7 | 0.98 | $C_{74}$ | $C_1$: 13408 | 2 | 34.0 | 1.18 | 58.5 | 1.09 |
| $C_{72}$ | $C_s$: 10528 | 2 | 77.3 | 0.32 | 0.0 | 0.39 | $C_{74}$ | $C_2$: 13290 | 2 | 37.7 | 0.79 | 51.9 | 0.73 |
| $C_{72}$ | $C_{2v}$: 11188 | 1 | 79.8 | 0.61 | 21.2 | 0.49 | $C_{74}$ | $C_2$: 13291 | 2 | 54.1 | 0.87 | 63.1 | 0.88 |
| $C_{72}$ | $C_1$: 10518 | 3 | 99.8 | 0.82 | 40.5 | 0.87 | $C_{74}$ | $C_2$: 13292 | 2 | 69.9 | 0.94 | 70.7 | 0.75 |
| $C_{72}$ | $C_1$: 10468 | 3 | 100.2 | 1.12 | 48.9 | 1.10 | $C_{74}$ | $C_1$: 13391 | 2 | 70.7 | 0.84 | 98.5 | 0.80 |
| $C_{72}$ | $C_1$: 10557 | 2 | 101.8 | 0.73 | 107.7 | 0.82 | $C_{74}$ | $C_3$: 13492 | 3 | 71.7 | 1.10 | 9.9 | 1.14 |
| $C_{72}$ | $C_2$: 10612 | 1 | 104.9 | 0.54 | 36.9 | 0.59 | $C_{74}$ | $C_{2v}$: 14239 | 2 | 86.9 | 0.77 | 0.0 | 0.77 |
| $C_{72}$ | $C_2$: 10626 | 2 | 107.9 | 0.63 | 116.6 | 0.67 | $C_{74}$ | $C_1$: 13384 | 2 | 89.1 | 0.45 | 104.4 | 0.38 |
| $C_{72}$ | $C_1$: 10526 | 3 | 117.3 | 0.79 | 55.6 | 0.81 | $C_{74}$ | $C_s$: 13336 | 2 | 97.8 | 0.57 | 50.4 | 0.57 |
| $C_{72}$ | $C_2$: 10693 | 2 | 118.8 | 0.59 | 53.5 | 0.60 | $C_{74}$ | $C_1$: 13479 | 3 | 99.3 | 1.07 | 38.4 | 0.99 |
| $C_{72}$ | $C_1$: 10688 | 3 | 121.6 | 0.74 | 56.6 | 0.77 | $C_{74}$ | $C_2$: 13961 | 2 | 100.9 | 1.24 | 132.1 | 1.05 |
| $C_{72}$ | $C_1$: 10469 | 3 | 122.2 | 0.85 | 70.9 | 0.78 | $C_{74}$ | $C_1$: 13771 | 2 | 101.3 | 0.58 | 57.1 | 0.62 |
| $C_{72}$ | $C_1$: 10774 | 3 | 125.8 | 1.03 | 40.9 | 0.95 | $C_{74}$ | $C_1$: 13549 | 2 | 105.2 | 0.58 | 49.6 | 0.55 |
| $C_{72}$ | $C_1$: 10615 | 2 | 127.9 | 0.57 | 66.5 | 0.63 | $C_{74}$ | $C_1$: 13410 | 2 | 108.6 | 0.82 | 74.9 | 0.91 |
| $C_{72}$ | $C_2$: 10554 | 2 | 131.7 | 0.57 | 148.1 | 0.58 | $C_{74}$ | $C_1$: 13393 | 1 | 116.4 | 0.52 | 65.7 | 0.50 |
| $C_{72}$ | $C_1$: 10849 | 2 | 134.1 | 0.60 | 132.1 | 0.59 | $C_{74}$ | $C_1$: 13334 | 2 | 118.1 | 0.29 | 72.7 | 0.30 |
| $C_{72}$ | $C_1$: 10538 | 2 | 135.4 | 0.37 | 51.2 | 0.36 | $C_{74}$ | $C_1$: 14049 | 1 | 119.5 | 0.58 | 47.1 | 0.53 |

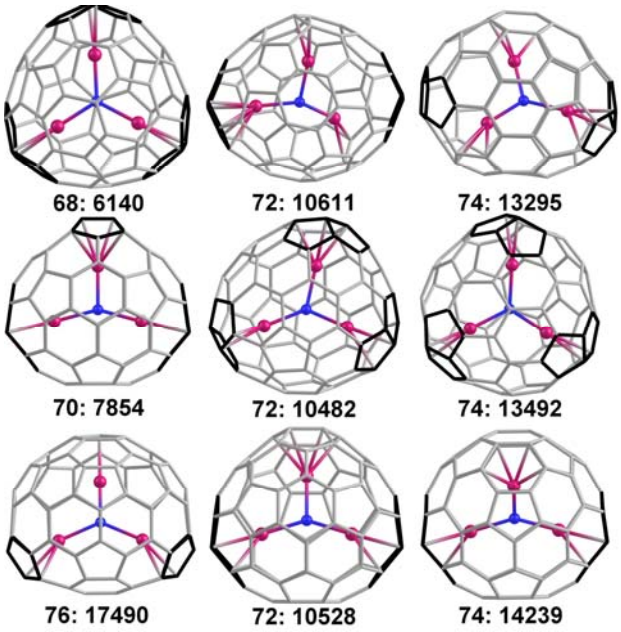


**Figure 1.** Molecular structures of selected $Sc_3N@C_{2n}$ isomers with $2n$ = 68–76 (C – gray, N – blue, Sc – pink, APPs are highlighted in black). Sc–C distances shorter than 2.350 Å are shown as bonds.

the empty fullerenes. For instance, the relative energy of the $Sc_3N@C_{68}$ isomer based on the $C_{2v}$: 6073 cage is found to be 246.0 kJ/mol, and this isomer is substantially less stable than many other $Sc_3N@C_{68}$ isomers, though for the empty $C_{68}^{6-}$ this cage is the second among the most stable ones (note also that the isomers $C_{2v}$: 6073 was also proposed for $Sc_2C_2@C_{68}$[28]). Such a high relative energy may be explained by the unfavorable location of APPs, so that the cluster, the shape of which follows to some extent the location of APPs, is strongly distorted from equilateral shape, with one of the Sc–N–Sc angles being 163.2º, and two others being equal to 98.4º. Besides, one of the Sc–N bonds in $Sc_3N@C_{68}$ ($C_{2v}$: 6073) is 1.918 Å, which is much shorter than the optimum Sc–N bondlength of ca 2.05 Å (see Discussion section). The $Sc_3N$ cluster retains almost equilateral shape inside the $C_2$: 6118 and $C_1$: 6138 cages, while Sc–N distances are 1.98–2.00 Å (compare to 1.993 Å in $D_3$: 6140), and these isomers are the second and the third most stable isomer of $Sc_3N@C_{68}$, with the stability order resembling that of the empty cages. HOMO-LUMO gaps of $Sc_3N@C_{68}$ isomers are almost equal to those of the empty $C_{68}^{6-}$ anions. All other isomers of $Sc_3N@C_{68}$ studied by DFT are at least by 71.4 kJ/mol less stable than the isomer $D_3$: 6140. Finally, our theoretical prediction of the highest stability of $Sc_3N@C_{68}$ ($D_3$: 6140) agrees well with the results of the single-crystal X-ray study,[6] which proved experimentally the $D_3$: 6140 cage isomer for the isolated $Sc_3N@C_{68}$.

The $C_{68}$ cage appears to be too small for the $Y_3N$ cluster, so that the cluster is forced to be pyramidal ($h$ = 0.550 Å) in the DFT-optimized structure of $Y_3N@C_{68}$ ($D_3$: 6140). Pyramidalization of the cluster points to the high strain in the structure, which is therefore energetically unfavorable,[39] and hence $M_3N@C_{68}$ with a uniform $M_3N$ cluster and M other than Sc has never been observed experimentally. However, the isolation of the mixed clusterfullerenes $ErSc_2N@C_{68}$ and $Er_2ScN@C_{68}$ was reported by Stevenson et al.[5]

**$M_3N@C_{70}$.** The study of $C_{70}^{6-}$ and $Sc_3N@C_{70}$ isomers was reported by us recently.[11] In brief, the most stable $C_{70}^{6-}$ isomer is $C_{2v}$: 7854 with three APPs, which is by 43 kJ/mol more stable than $C_{70}^{6-}$ based on the sole IPR isomer of $C_{70}$, $D_{5h}$: 8149. The HOMO-LUMO gap of $C_{2v}$:7854, 1.24 eV, is the largest among the most stable $C_{70}^{6-}$ isomers, none of which has a gap higher than 1.00 eV. The stability

of $C_{2v}$: 7854 isomer with respect to the IPR cage is further enhanced once the $Sc_3N$ cluster is encapsulated into the fullerene: $Sc_3N@C_{70}$ ($C_{2v}$: 7854) is 164 kJ/mol more stable than $Sc_3N@C_{70}$ ($D_{5h}$: 8149). The cluster in $Sc_3N@C_{70}$ ($C_{2v}$: 7854) is planar and significantly distorted from equilateral shape (Sc–N–Sc angles are 150.0º and 105.0º, see Fig. 1). However, this is still the lowest energy isomers as in all other low-energy $C_{70}^{6-}$ cages either a stronger distortion of the cluster is observed, or one of the APPs remains uncoordinated. Finally, the DFT-computed HOMO-LUMO gap and the IR spectra of $Sc_3N@C_{70}$ ($C_{2v}$: 7854) matched those of the experimentally isolated $Sc_3N@C_{70}$, thus justifying the assignment of the latter to the $C_{2v}$: 7854 cage isomer.[11] Similar to $Y_3N@C_{68}$, the $Y_3N$ cluster is still too large for this cage size, and in $Y_3N@C_{70}$ ($C_{2v}$: 7854) the cluster is predicted to be pyramidal ($h$ = 0.340 Å).

**$M_3N@C_{72}$.** The isomer $D_2$: 10611 with two APPs is found to be the lowest energy isomer of $C_{72}^{6-}$, while the other structures are less stable by at least 69 kJ/mol. Specifically, the only IPR isomer of $C_{72}$, $D_{6d}$: 11190, is 226.2 kJ/mol less stable in the hexaanionic state than $D_2$: 10611. The HOMO-LUMO gap of $D_2$: 10611, 1.12 eV, is among the largest gaps for the 20 lowest energy isomers of $C_{72}^{6-}$, and only three other isomers in this set have their HOMO-LUMO gaps higher than 1 eV: $C_1$: 10482 (1.01 eV), $C_1$: 10468 (1.12 eV), and $C_1$: 10774 (1.03 eV).

The stability order of the $Sc_3N@C_{72}$ isomers is drastically different from that of the empty $C_{72}^{6-}$ hexaanions. The most stable isomer has the $C_s$: 10528 cage and a HOMO-LUMO gap of 0.39 eV. The second and the third most stable isomers are $C_{2v}$: 11188 ($\Delta E$=21.2 kJ/mol, gap 0.49 eV) and $C_1$: 10482 ($\Delta E$=26.7 kJ/mol, gap 0.98 eV), while the structure with the $D_2$: 10611 cage is by 54.6 kJ/mol less stable than the $C_s$: 10528 isomer and has a gap of 0.89 eV, which is by 0.23 eV smaller than the gap predicted for the same isomer of $C_{72}^{6-}$. The reason for these changes in the relative stability of the $Sc_3N@C_{72}$ isomers becomes obvious when the location of APPs on the cage is analyzed for each structure (Fig. 1). The isomer $D_2$: 10611 has an elongated shape, and two APPs are located at the poles of the fullerene. Hence, there is no way for $Sc_3N$ to coordinate the two APPs at once, unless the cluster is severely distorted from the equilateral shape, and in the optimized structure of $Sc_3N@C_{72}$ ($D_2$: 10611)

one of the APPs remains unstabilized. On the contrary, the location of APPs in $C_s$: 10528, $C_{2v}$: 11188 and $C_1$: 10482 isomers is more favorable for their efficient stabilization by the coordination to Sc atoms. However, even in these most stable isomers the cluster geometry is still significantly distorted from the symmetric configuration. In $C_{2v}$: 11188 and $C_1$: 10482 isomers the cluster is forced to be pyramidal (displacements of nitrogen atom out of the $Sc_3$ plane are 0.155 and 0.208 Å, respectively); moreover, the cluster is significantly distorted from $C_3$ symmetry inside $C_1$: 10482, one of the Sc–N–Sc angles being 132.5º. The cluster is almost planar ($h$=0.022 Å) in the $C_s$: 10528 isomer, but distortion from the equilateral shape is even stronger: one Sc–N–Sc angle is 144.8º, while two others are 107.6º.

For $Y_3N@C_{72}$ we have studied the $C_s$: 10528 isomer because of its highest stability for $Sc_3N@C_{72}$, and the $C_1$: 10482 and $C_1$: 10468 isomers because of the relatively high HOMO-LUMO gaps of these cages in $C_{72}^{6-}$ as well as in $Sc_3N@C_{72}$. The stability order is different from that predicted for $Sc_3N@C_{72}$. $Y_3N@C_{72}$ ($C_1$: 10482) is the most stable isomer among the three studied structures. In the $C_1$: 10482 and $C_s$: 10528 isomers the $Y_3N$ cluster is pyramidal ($h$ = 0.446 and 0.325 Å, respectively). In $Y_3N@C_{72}$ ($C_1$: 10468) the cluster is close to the planarity ($h$ = 0.053 Å), but is severely distorted from the three-fold symmetry with two Y–N–Y angles having abnormal values (140.1º and 99.1º). These structural and energetic reasons clearly indicate why it was not possible to isolate a $C_{72}$ nitride cluster structure in our extended experimental studies.

**$M_3N@C_{74}$.** The correlation between the relative stabilities of $Sc_3N@C_{74}$ and $C_{74}^{6-}$ isomers resembles the situation described above for $C_{72}$ cage. The most stable isomer of $C_{74}^{6-}$, $C_2$: 13295, has two APPs which are located almost on the opposite poles of the fullerene. As a result, the encapsulated cluster cannot efficiently stabilize two APPs, leaving one of them uncoordinated (Fig. 1). The relative energy of $Sc_3N@C_{74}$ ($C_2$: 13295) is 18.7 kJ/mol, while the most stable isomer of $Sc_3N@C_{74}$ is based on the $C_{2v}$: 14239 cage (Fig. 1), which in the $C_{74}^{6-}$ state is by 87 kJ/mol less stable than $C_{74}^{6-}$ ($C_2$: 13295). In $Sc_3N@C_{74}$ ($C_{2v}$: 14239), which obeys $C_s$ symmetry, the cluster is slightly pyramidal ($h$ = 0.151 Å) and significantly distorted from the three-fold symmetry: one of Sc–N–Sc angles is 146.2º and two others are 105.9º.

The second most stable isomer of $Sc_3N@C_{74}$, $C_3$: 13492 (Fig. 1), is also based on the relatively unstable cage ($\Delta E$ = 71.7 kJ/mol for $C_{74}^{6-}$). This isomer has three APPs and the largest HOMO-LUMO gap (1.10 eV in $C_{74}^{6-}$, 1.14 eV in $Sc_3N@C_{74}$) among 20 the most stable cages. The APPs are located around the equator of the cage and closer to one of the poles. The cluster follows the $C_3$ symmetry of the cage, while the Sc atoms of the $Sc_3N$ cluster are coordinated to APPs and the cluster is pyramidal ($h$ = 0.329 Å). Computations of $Y_3N@C_{74}$ isomers were performed only for $C_2$: 13295, $C_3$: 13492, and $C_{2v}$: 14239 cages. Their relative stability is significantly altered compared to $Sc_3N@C_{74}$ isomers: the most stable $Y_3N@C_{74}$ isomer is based on the $C_3$: 13492 cage, while $C_2$: 13295 and $C_{2v}$: 14239 isomers are 52.1 and 86.8 kJ/mol less stable. The cluster is pyramidal in all optimized $Y_3N@C_{74}$ molecules, $h$ = 0.568 Å, 0.088 Å and 0.573 Å in $C_3$: 13492, $C_2$: 13295 and $C_{2v}$: 14239 isomers, respectively, and in the latter two isomers it is also significantly distorted similar to the distortion of the $Sc_3N$ cluster in the corresponding $Sc_3N@C_{74}$ structures described above. These findings support the fact that an isolation of a stable $C_{74}$ nitride cluster fullerene was not successful up till now.

**$M_3N@C_{76}$.** $C_{76}$ has two IPR isomers. In the hexaanionic form one of them, $T_d$: 19151 is the third most stable isomer with the relative energy of 20.8 kJ/mol, but it has a very low HOMO-LUMO gap (0.14 eV). Another IPR isomer, $D_2$: 19150, has a gap of 0.75 eV and is by 101.0 kJ/mol less stable than the most stable structure, the non-IPR isomer $C_s$: 17490 with two APPs and a HOMO-LUMO gap of 1.12 eV. Significantly, seven structures from the list of ten most stable $C_{76}^{6-}$ isomers have two APPs, two isomers have only one APP, and there are no stable isomers with three APPs.

When $Sc_3N$ is encapsulated inside $C_{76}$, DFT predicts the most stable isomer to be the $T_d$: 19151 cage, but this isomer has a small gap (0.16 eV) as in the empty hexaanion $C_{76}^{6-}$. The second most stable isomer of $Sc_3N@C_{76}$ has the $C_s$: 17490 cage (Fig. 1) and a HOMO-LUMO gap of 1.08 eV. Hence this structure might be a suitable candidate for the stable $Sc_3N@C_{76}$ clusterfullerene. The cluster inside this cage is planar, and though it is distorted from a three-fold symmetry (Sc–N–Sc angles are 133.3º and 113.1º). These distortions are not as strong as in the lowest energy isomers of $Sc_3N@C_{72}$ and $Sc_3N@C_{74}$ clusterfullerenes discussed above. The interesting feature of the cluster geometry in $Sc_3N@C_{76}$ ($C_s$:

17490) is that two of the Sc–N bonds are rather long (2.113 Å, which may be compared to 2.034 Å in $Sc_3N@C_{80}$ discussed below), while the third bond is very short (1.984 Å, that is much shorter than 1.993 Å in $Sc_3N@C_{68}$ and comparable to one of the Sc–N bonds in $Sc_3N@C_{70}$, 1.987 Å, which is the shortest Sc–N bond predicted by DFT for experimentally isolated $Sc_3N$ clusterfullerenes).

The increase of the cluster size by replacing $Sc_3N$ to $Y_3N$ results in significant changes in the relative stability of different cage isomers. The most stable isomer of $Y_3N@C_{76}$ is $C_s$: 17490, while $T_d$: 19151 is less stable by 37.7 kJ/mol. The reason for such a change in stability may be explained by the different size and shape of the cavity inside the cage, which can be occupied by the cluster. The cage of the $T_d$: 19151 isomer appears to be too small for the $Y_3N$ cluster, and the latter is significantly pyramidalized ($h$ = 0.639 Å). On the contrary, the $C_s$: 17490 cage is more suitable for this cluster size, and the degree of the cluster pyramidalization is much lower ($h$ = 0.255 Å). For the same reason the isomer $C_s$: 18161, being rather unstable as $C_{76}^{6-}$ and as $Sc_3N@C_{76}$ ($\Delta E$ = 64.7 and 70.0 kJ/mol, respectively), becomes the second most stable isomer for $Y_3N@C_{76}$ ($\Delta E$ = 26.1 kJ/mol). The cage of the $C_s$: 18161 isomer has such a size and shape that the encapsulated $Y_3N$ cluster remains planar.

Experimentally $M_3N@C_{76}$ has not been isolated for any homogenious $M_3N$ cluster. $Dy_3N@C_{76}$ was observed by mass-spectrometry in the crude product of the synthesis of $Dy_3N@C_{2n}$ clusterfullerenes,[21] but its amount was not sufficient yet for an isolation of this compound and for its spectroscopic characterization. Results of this work show that this clusterfullerene most probably has the $C_s$: 17490 cage isomer. The asymmetric cluster configuration in this structure seems to be favorable for the formation of the mixed $Sc_xM_{3-x}N@C_{76}$ clusterfullerenes.

**$M_3N@C_{78}$.** The study of $C_{78}^{6-}$ and $M_3N@C_{78}$ (M = Sc, Y, La, Lu) isomers was reported by us recently.[39] In brief, the most stable $C_{78}^{6-}$ isomer is IPR $D_{3h}$: 24109 (gap 1.21 eV), which is followed by the non-IPR isomer $C_2$: 22010 ($\Delta E$ = 59.1 kJ/mol, gap 1.60 eV) with two APPs. The relative stability order found for $C_{78}^{6-}$ was preserved for the $Sc_3N@C_{78}$ isomers in agreement with experimental isolation of $Sc_3N@C_{78}$ with IPR $D_{3h}$: 24109 cage.[7] However, with the larger $Y_3N$ cluster inside, the $C_2$: 22010

***Table 3.*** Relative energies (Δ*E*, kJ/mol), HOMO-LUMO gaps (gap, eV), and binding energies (BE-2, eV) of the most stable $C_{2n}^{6-}$ and $M_3N@C_{2n}$ (2*n* = 76, 80, 82, 84, 86, 88; M = Sc, Y) isomers as computed at the DFT level

| | | | $C_{2n}^{6-}$ | | $Sc_3N@C_{2n}$ | | $Y_3N@C_{2n}$ | | | Cage | | $C_{2n}^{6-}$ | | $Sc_3N@C_{2n}$ | | $Y_3N@C_{2n}$ | |
|---|---|---|---|---|---|---|---|---|---|---|---|---|---|---|---|---|---|
| $C_{2n}$ | isomer | APPs | Δ*E* | gap | Δ*E* | gap | Δ*E* | gap | $C_{2n}$ | isomer | APPs | Δ*E* | gap | Δ*E* | gap | Δ*E* | gap |
| $C_{76}$ | $C_s$: 17490 | 2 | 0.0 | 1.12 | 20.0 | 1.08 | 0.0 | 1.24 | $C_{80}$ | $I_h$: 31924 | 0 | 0.0 | 1.83 | 0.0 | 1.46 | 0.0 | 1.54 |
| $C_{76}$ | $C_{2v}$: 19138 | 1 | 16.8 | 0.78 | 41.7 | 0.80 | 103.2 | 0.97 | $C_{80}$ | $D_{5h}$: 31923 | 0 | 88.2 | 1.51 | 67.0 | 1.33 | 70.2 | 1.40 |
| $C_{76}$ | $T_d$: 19151 | 0 | 20.8 | 0.14 | 0.0 | 0.16 | 37.7 | 0.10 | $C_{80}$ | $C_{2v}$: 31922 | 0 | 196.7 | 0.61 | 166.5 | 0.67 | 93.9 | 0.67 |
| $C_{76}$ | $C_1$: 17465 | 2 | 53.9 | 0.89 | 83.1 | 0.90 | 55.4 | 0.90 | $C_{80}$ | $C_1$: 31891 | 1 | 246.9 | 0.99 | 185.1 | 0.92 | 149.8 | 0.97 |
| $C_{76}$ | $C_2$: 17765 | 2 | 55.8 | 1.37 | 116.4 | 1.13 | 80.2 | 1.29 | $C_{80}$ | $C_1$: 28325 | 2 | 262.8 | 1.36 | 227.4 | 1.17 | 90.0 | 1.24 |
| $C_{76}$ | $C_2$: 17512 | 2 | 60.1 | 1.14 | 176.6 | 1.02 | 71.1 | 1.15 | $C_{80}$ | $C_1$: 28319 | 1 | 285.6 | 0.74 | 239.7 | 0.84 | 145.2 | 0.84 |
| $C_{76}$ | $C_2$: 18161 | 2 | 64.7 | 1.12 | 70.0 | 1.13 | 26.1 | 1.20 | $C_{80}$ | $C_2$: 29591 | 2 | 288.4 | 1.33 | 255.4 | 1.20 | 110.6 | 1.41 |
| $C_{76}$ | $C_1$: 17588 | 2 | 78.7 | 0.85 | 81.1 | 0.75 | 85.7 | 0.84 | $C_{80}$ | $C_1$: 28324 | 1 | 295.3 | 0.47 | 261.4 | 0.45 | 168.5 | 0.46 |
| $C_{76}$ | $C_1$: 17760 | 2 | 79.9 | 1.07 | 95.7 | 0.91 | 83.7 | 0.98 | $C_{80}$ | $C_{2v}$: 31920 | 0 | 301.8 | 0.58 | 290.5 | 0.53 | 124.5 | 0.63 |
| $C_{76}$ | $C_1$: 17459 | 1 | 80.5 | 0.54 | 106.2 | 0.45 | 149.7 | 0.54 | $C_{80}$ | $C_1$:31876 | 1 | 300.0 | 0.50 | 232.1 | 0.47 | 144.2 | 0.46 |
| $C_{82}$ | $C_{2v}$: 39718 | 0 | 0.0 | 0.79 | 0.0 | 0.83 | 29.6 | 0.84 | $C_{84}$ | $D_2$: 51589 | 0 | 0.0 | 0.80 | 13.8 | 0.80 | 33.2 | 0.90 |
| $C_{82}$ | $C_{2v}$: 39705 | 1 | 30.1 | 1.32 | 17.7 | 1.20 | 0.0 | 1.32 | $C_{84}$ | $C_s$:51365 | 1 | 1.8 | 1.34 | 0.0 | 1.10 | 0.0 | 1.34 |
| $C_{82}$ | $C_{3v}$: 39717 | 0 | 48.9 | 0.22 | 58.1 | 0.21 | 119.1 | 0.19 | $C_{84}$ | $D_{2d}$: 51591 | 0 | 29.7 | 0.77 | 18.0 | 0.75 | 48.8 | 0.82 |
| $C_{82}$ | $C_s$: 39715 | 0 | 54.0 | 0.54 | 41.2 | 0.55 | 51.0 | 0.50 | $C_{84}$ | $C_s$: 51578 | 0 | 36.9 | 0.65 | 43.4 | 0.67 | 49.3 | 0.66 |
| $C_{82}$ | $C_s$: 39663 | 1 | 61.2 | 1.42 | 49.8 | 1.03 | 32.6 | 1.51 | $C_{84}$ | $C_s$: 51583 | 0 | 37.9 | 0.89 | 43.5 | 0.76 | 60.7 | 0.82 |
| $C_{82}$ | $C_2$: 39714 | 0 | 87.4 | 0.84 | 89.5 | 0.61 | 54.4 | 0.64 | $C_{84}$ | $D_2$: 51590 | 0 | 38.5 | 0.59 | 39.0 | 0.70 | 77.3 | 0.68 |
| $C_{82}$ | $C_s$: 39704 | 1 | 111.1 | 0.83 | 94.2 | 0.79 | 103.2 | 0.87 | $C_{84}$ | $C_{2v}$: 51575 | 0 | 48.6 | 0.64 | 31.8 | 0.68 | 73.4 | 0.70 |
| $C_{82}$ | $C_s$: 36652 | 2 | 118.1 | 1.25 | 146.7 | 0.94 | 65.1 | 1.26 | $C_{84}$ | $C_2$: 50322 | 1 | 55.5 | 1.37 | 83.1 | 0.83 | 68.1 | 1.23 |
| $C_{82}$ | $C_1$: 39656 | 1 | 139.0 | 0.67 | 147.8 | 0.56 | 104.2 | 0.65 | $C_{84}$ | $C_1$: 51350 | 1 | 59.3 | 1.16 | 70.8 | 0.90 | 63.0 | 1.13 |
| $C_{82}$ | $C_s$: 39713 | 0 | 132.1 | 0.58 | 118.8 | 0.49 | 104.0 | 0.50 | $C_{84}$ | $C_s$: 51425 | 1 | 63.1 | 0.99 | 57.0 | 0.91 | 58.9 | 1.01 |
| $C_{86}$ | $D_3$: 63761 | 0 | 0.0 | 1.51 | 12.2 | 1.13 | 3.7 | 1.47 | $C_{88}$ | $D_2$: 81738 | 0 | 0.0 | 0.97 | 0.0 | 0.81 | 0.0 | 0.99 |
| $C_{86}$ | $C_{2v}$: 63751 | 0 | 35.7 | 0.44 | 28.6 | 0.53 | 0.0 | 0.56 | $C_{88}$ | $C_s$: 81735 | 0 | 70.6 | 0.61 | 64.5 | 0.49 | 55.5 | 0.74 |
| $C_{86}$ | $C_s$: 63757 | 0 | 56.0 | 0.68 | 0.0 | 0.63 | 26.1 | 0.66 | $C_{88}$ | $C_s$: 81734 | 0 | 78.6 | 0.85 | 60.9 | 0.53 | 77.4 | 0.88 |
| $C_{86}$ | $C_1$: 58832 | 1 | 71.5 | 0.87 | 45.8 | 0.80 | 40.8 | 0.89 | $C_{88}$ | $C_1$: 81733 | 0 | 89.2 | 0.59 | 58.0 | 0.66 | 91.3 | 0.62 |
| $C_{86}$ | $C_1$: 63755 | 0 | 72.6 | 0.67 | 33.5 | 0.68 | 34.6 | 0.69 | $C_{88}$ | $C_1$: 81729 | 0 | 89.9 | 0.36 | 63.3 | 0.53 | 86.9 | 0.38 |
| $C_{86}$ | $C_1$: 63291 | 1 | 79.6 | 1.06 | 51.3 | 0.75 | 54.9 | 1.05 | $C_{88}$ | $C_1$: 80982 | 1 | 96.8 | 1.13 | 57.2 | 0.93 | 78.3 | 1.18 |
| $C_{86}$ | $C_2$: 63339 | 1 | 94.6 | 0.92 | 48.0 | 0.72 | 56.2 | 0.86 | $C_{88}$ | $C_2$: 81731 | 0 | 96.9 | 0.67 | 86.1 | 0.63 | 86.9 | 0.76 |
| $C_{86}$ | $C_2$: 63229 | 1 | 98.3 | 1.27 | 87.9 | 0.97 | 69.5 | 1.34 | $C_{88}$ | $C_1$: 69747 | 1 | 101.5 | 0.97 | 80.1 | 0.78 | 75.5 | 0.97 |
| $C_{86}$ | $C_2$: 63756 | 0 | 103.8 | 0.45 | 44.9 | 0.43 | 84.5 | 0.42 | $C_{88}$ | $C_s$: 81712 | 0 | 103.4 | 0.51 | 43.2 | 0.54 | 76.1 | 0.53 |
| $C_{86}$ | $C_s$: 63750 | 0 | 106.7 | 0.19 | 80.6 | 0.30 | 87.7 | 0.23 | $C_{88}$ | $C_1$: 70333 | 1 | 105.9 | 0.85 | 105.0 | 0.41 | 79.3 | 0.82 |

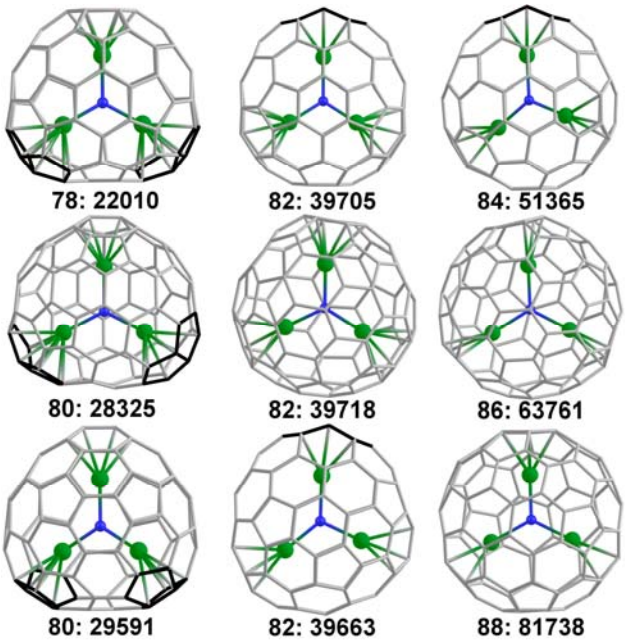


**Figure 2.** Molecular structures of selected $Y_3N@C_{2n}$ isomers with $2n$ = 78–86 (C – gray, N – blue, Y – green, APPs are highlighted in black). Y–C distances shorter than 2.550 Å are shown as bonds.

cage (Fig. 2) becomes the most stable one, being by 83.6 kJ/mol lower in energy than the $D_{3h}$: 24109 isomer. When switching from $Sc_3N$ to $Y_3N$, a dramatic change in the stability of the cage isomers can be explained by an unsuitable size of the $D_{3h}$: 24109 cage, which forces the encapsulated $Y_3N$ cluster to be pyramidal ($h$ = 0.554 Å). On the contrary, the $Y_3N$ cluster has enough space to be planar inside the $C_2$: 22010 isomer. For the same reason, two other non-IPR isomers of $Y_3N@C_{78}$, $C_1$: 21975 ($\Delta E$ = 65.1 kJ/mol, gap 1.21 eV) and $C_1$: 22646 ($\Delta E$ = 67.5 kJ/mol, gap 1.26 eV) are also more stable than $Y_3N@C_{78}$ ($D_{3h}$: 24109).

Experimental spectroscopic studies of the recently isolated $Tm_3N@C_{78}$[13] and the major isomer of $Dy_3N@C_{78}$[39] have shown that their carbon cages are different from that of $Sc_3N@C_{78}$. DFT-computed vibrational spectrum of $Y_3N@C_{78}$ ($C_2$: 22010) showed perfect agreement to the experimental spectra of $Dy_3N@C_{78}$ and $Tm_3N@C_{78}$ hence proving the assignment of the cage structure of these clusterfullerenes to the $C_2$: 22010 cage in agreement with the DFT-predicted higher stability of the latter.[39]

**$M_3N@C_{80}$.** The three lowest energy isomers of $C_{80}^{6-}$ are IPR structures: the most stable one, $I_h$: 31924, is 88.2 kJ/mol more stable than $D_{5h}$: 31923, which in due turn is by 108.5 kJ/mol more stable than the following $C_{2v}$: 31922 isomer. The fourth isomer, the non-IPR $C_1$: 31891 with one APP, is by 247 kJ/mol less stable than $I_h$: 31924. Besides a remarkable stability, the two first isomers also have a large HOMO-LUMO gap (1.83 and 1.51 eV, respectively), and can therefore be regarded as suitable cages for the formation of nitride clusterfullerenes. Indeed, $M_3N@C_{80}$ based on $I_h$: 31924 and $D_{5h}$: 31923 cages (also referred in the literature as isomers I and II) are the most abundant clusterfullerenes for any M.

The order of isomer stability for $Sc_3N@C_{80}$ follows that for $C_{80}^{6-}$, albeit the energy difference between the three first structures and the others are smaller than those for empty cages. The difference between $Sc_3N@C_{80}$ ($I_h$: 31924) and $Sc_3N@C_{80}$ ($D_{5h}$: 31924) is 67.0 kJ/mol, and the $C_1$: 31922 isomer is by 166.5 kJ/mol less stable than $I_h$: 31924 (*versus* 246.9 kJ/mol for empty $C_{80}^{6-}$). For $Y_3N@C_{80}$ the energy gap between IPR and non-IPR structures is further diminished. The isomers $I_h$: 31924 and $D_{5h}$:

31924 are still the most stable ones, but the third most stable isomer is $C_1$: 28325 (Fig. 2), which has two APPs and the gap of 1.24 eV. While this isomer is less stable than $I_h$: 31924 by 262.8 and 227.4 kJ/mol for $C_{80}^{6-}$ and $Sc_3N@C_{80}$, respectively, for $Y_3N@C_{80}$ its relative energy is only 90.0 kJ/mol, being slightly lower than for the IPR $C_{2v}$: 31922 (the third isomer in stability order for $C_{80}^{6-}$ and $Sc_3N@C_{80}$). In agreement with the results of these calculations, only two isomers are known for $Sc_3N@C_{80}$, but for $Dy_3N@C_{80}$ Yang et al.[15] have recently reported the isolation of the third isomer, albeit in much smaller yield. The authors have found that the onset in the absorption spectrum of $Dy_3N@C_{80}$ (III) is at 1.31 eV, close that of $Dy_3N@C_{80}$ (II), and based on the results of our calculations the non-IPR $C_1$: 28325 or $C_2$: 29591 cage isomers (Fig. 2) are energetically favored for $Dy_3N@C_{80}$ (III).

A significant stabilization of the other cage isomers with respect to $I_h$: 31924 and $D_{5h}$: 31923 cages for $Y_3N@C_{80}$ may be understood if the cage and the cluster size are analyzed. The difference between the isomers is most apparent when Y–N distances are compared, namely, 2.060 Å in $I_h$: 31924 (the cluster has $C_3$ symmetry in this isomer), 2.104/2.148/2.153 Å in $C_1$: 28325 and 2.111/2.146/2.146 Å in $C_2$: 29591. It appears that the cluster is constrained in $I_h$: 31924 and has more space in the other isomers, which results in a lengthening of the Y–N bonds by 0.04 – 0.09 Å in $C_1$: 28325 or $C_2$: 29591 isomers of $Y_3N@C_{80}$ compared to $I_h$: 31924. Noteworthily, $Y_3N$ is slightly pyramidal in the pyrrolidine adduct of $Y_3N@C_{80}$,[47] and $Dy_3N$, which has a similar size to $Y_3N$, is the largest $M_3N$ cluster known to be nearly-planar inside $C_{80}$ ($I_h$: 31924).[25] Hence, it may be expected that the strain caused by the insufficient inner size of the cage for $M_3N$ cluster is rather high for the $I_h$: 31924 cage, and the larger $Tb_3N$ and $Gd_3N$ clusters are forced to be pyramidal in $M_3N@C_{80}$ ($I_h$: 31924) as shown by single crystal X-ray diffraction studies.[17, 23]

**$M_3N@C_{82}$.** Among the ten most stable isomers of $C_{82}^{6-}$, five obey the IPR, including the most stable $C_{2v}$: 39718 isomer. However, only non-IPR isomers have HOMO-LUMO gaps above 1 eV, namely $C_{2v}$: 39705 ($\Delta E$ = 30.1 kJ/mol, gap 1.32 eV), $C_s$: 39663 ($\Delta E$ = 61.2 kJ/mol, gap 1.42 eV), and $C_2$: 36652 ($\Delta E$ = 118.1 kJ/mol, gap 1.25 eV). The stability order of these isomers found for $C_{82}^{6-}$ is mostly preserved for $Sc_3N@C_{82}$, however the $C_{2v}$: 39705 isomer is stabilized relative to the $C_{2v}$: 39718 cage ($\Delta E$ = 17.7

kJ/mol versus 30.1 kJ/mol for the $C_{82}^{6-}$). The HOMO-LUMO gaps of the $C_s$: 39663 and $C_2$: 36652 isomers of $Sc_3N@C_{82}$ are significantly smaller than in $C_{82}^{6-}$ which probably points to the less effective cluster-cage interactions than in $Sc_3N@C_{82}$ ($C_{2v}$: 39705) or in the smaller cages described above, in which the gaps of $Sc_3N@C_{2n}$ are usually similar to those of $C_{2n}^{6-}$. Thus, for $Sc_3N@C_{82}$, if isolated at all, the $C_{2v}$: 39705 isomer may be suggested as the most probable structure based on its thermodynamic stability and large HOMO-LUMO gap.

The stability order of $Y_3N@C_{82}$ isomers is significantly altered compared to $Sc_3N@C_{82}$ or $C_{82}^{6-}$. The most stable isomer of $Y_3N@C_{82}$ is $C_{2v}$: 39705 (gap 1.32 eV), followed by $C_{2v}$: 39718 ($\Delta E$ = 29.6 kJ/mol, gap 0.84 eV) and the almost isoenergetic $C_s$: 39663 ($\Delta E$ = 32.6 kJ/mol, gap 1.51 eV) (Fig. 2). Note that contrary to $Sc_3N@C_{82}$, the band-gaps of the $C_s$: 39663 and $C_2$: 36652 isomers of $Y_3N@C_{82}$ are similar to $C_{82}^{6-}$. The analysis of the DFT optimized molecular structures of these isomers in comparison to their $Sc_3N@C_{82}$ analogues has shown that in the latter the $Sc_3N$ cluster is displaced toward one side of the cage, while $Y_3N$ is in a center position inside the fullerene. As a result, Sc and Y atoms are coordinated to different fragments of the cage, which apparently results in different efficiency of the cluster-cage interactions.

$M_3N@C_{82}$ (M = Tm and Dy) were isolated experimentally,[13, 21] and their UV-Vis absorption spectra are shown to be very similar pointing to the identical cage structures of these clusterfullerenes. However, structural studies of these compounds have not been reported yet. Both compounds have large optical gaps, exceeding 1.3 eV. Based on the results of this work, the isomers $C_{2v}$: 39705 and $C_s$: 39663 can be proposed as the most probable cage structures because of their high thermodynamic stability and the large HOMO-LUMO gap. Further spectroscopic or structural studies are required to favor one of these structures.

**$M_3N@C_{84}$.** The list of ten most stable isomers of $C_{84}^{6-}$ includes six IPR isomers and four isomers with one APP. As in the case of $C_{82}^{6-}$, the non-IPR isomers have higher HOMO-LUMO gaps; specifically, only the non-IPR isomers have HOMO-LUMO gaps higher than 1 eV, while the HOMO-LUMO gaps for IPR structures do not exceed 0.8 eV. The two most stable isomers, IPR $D_2$: 51589 and

non-IPR $C_s$: 51365 (Fig. 2), are essentially isoenergetic, however the much higher HOMO-LUMO gap of the non-IPR cage (1.34 eV *versus* 0.80 eV for IPR isomer) makes it a preferable candidate for the both thermodynamically and kinetically stable $M_3N@C_{84}$. For the $Sc_3N@C_{84}$ and $Y_3N@C_{84}$ series, this isomer is the most stable one, and its stabilization relative to the $D_2$: 51589 isomer in the $C_{84}^{6-}$ – $Sc_3N@C_{84}$ – $Y_3N@C_{84}$ sequence can be pointed out (Table 3). The HOMO-LUMO gaps of the $C_s$: 51365 and the non-IPR $C_1$: 51350 and $C_2$: 50322 isomers of $Sc_3N@C_{84}$ are significantly smaller than in the corresponding $C_{84}^{6-}$ or $Y_3N@C_{84}$ isomers. The analysis of their DFT optimized structures shows that, similar to the case of $M_3N@C_{82}$ discussed above, these fullerene are too large for a $Sc_3N$ cluster, and the latter has to be displaced to one of the parts of the fullerene cage to establish an interaction with the cage. On the contrary, the $Y_3N$ cluster resides in the center of $Y_3N@C_{84}$ cage, and hence the bonding sites for Sc are different from that of Y.

Experimentally $M_3N@C_{84}$ was isolated for M = Tm,[13] Dy[21] and Tb.[22] For $Tb_3N@C_{84}$ and $Dy_3N@C_{84}$ the second, less abundant isomer was also isolated in small amounts. The results of this work are in perfect agreement with X-ray crystallographic studies of the major isomer of $Tb_3N@C_{84}$, which is shown to have a $C_s$: 51365 cage.[22] Reliable spectroscopic and/or structural data are not available yet for the minor isomer of $M_3N@C_{84}$, but our results show that it might be based on the IPR $D_2$: 51589 cage (and in this case it should have a rather small band-gap and a low kinetic stability) or on one of the $C_s$: 51425, $C_1$: 51350 or $C_1$: 50322 isomers, which are almost isoenergetic and have band-gaps of 1.01, 1.13 and 1.23 eV, respectively.

**$M_3N@C_{86}$.** The most stable isomer of $C_{86}^{6-}$, $D_3$: 63761, obeys the IPR and has the largest HOMO-LUMO gap, 1.51 eV, among the ten lowest energy isomers of $C_{86}^{6-}$. As in the case of $C_{84}^{6-}$, the list of the most stable structures includes six IPR and four non-IPR isomers, all of the latter with one APP. For $Sc_3N@C_{86}$, the isomer $D_3$: 63761 is by 12.2 kJ/mol less stable than $C_s$: 63757, and it has a smaller HOMO-LUMO gap than the empty $C_{86}^{6-}$ for the same reason as discussed above for $Sc_3N@C_{82}$ and $Sc_3N@C_{84}$ isomers. For $Y_3N@C_{86}$, the isomer $D_3$: 63761 (Fig. 2) is also the second most stable one,

***Table 4.*** Relative energies ($\Delta E$, kJ/mol), HOMO-LUMO gaps (gap, eV), and binding energies (BE-2, eV) of the most stable $C_{2n}^{6-}$ and $Y_3N@C_{2n}$ ($2n$ = 90 – 98) isomers as computed at the DFT level

| $C_{2n}$ | Cage isomer | $C_{2n}^{6-}$ $\Delta E$ | gap | $C_{2n}$ | Cage isomer | $C_{2n}^{6-}$ $\Delta E$ | gap | $C_{2n}$ | Cage isomer | $C_{2n}^{6-}$ $\Delta E$ | gap | $C_{2n}$ | Cage isomer | $C_{2n}^{6-}$ $\Delta E$ | gap | $C_{2n}$ | Cage isomer | $C_{2n}^{6-}$ $\Delta E$ | gap |
|---|---|---|---|---|---|---|---|---|---|---|---|---|---|---|---|---|---|---|---|
| $C_{90}$ | $C_2$: 43 | 0.0 | 0.83 | $C_{92}$ | $D_3$: 85 | 0.0 | 0.63 | $C_{94}$ | $C_2$: 121 | 0.0 | 1.18 | $C_{96}$ | $D_2$: 186 | 0.0 | 1.06 | $C_{98}$ | $C_2$: 166 | 0.0 | 1.02 |
| $C_{90}$ | $C_2$: 44 | 13.5 | 0.81 | $C_{92}$ | $C_1$: 66 | 22.3 | 0.81 | $C_{94}$ | $C_2$: 117 | 19.2 | 0.71 | $C_{96}$ | $C_2$: 158 | 28.0 | 0.87 | $C_{98}$ | $C_1$: 247 | 16.1 | 0.99 |
| $C_{90}$ | $C_1$: 21 | 39.2 | 0.67 | $C_{92}$ | $T$: 86 | 24.2 | 1.47 | $C_{94}$ | $C_2$: 126 | 36.4 | 0.92 | $C_{96}$ | $D_{6d}$: 187 | 54.2 | 1.50 | $C_{98}$ | $C_2$: 252 | 29.8 | 0.97 |
| $C_{90}$ | $C_2$: 42 | 39.8 | 0.77 | $C_{92}$ | $C_2$: 65 | 28.6 | 1.06 | $C_{94}$ | $C_2$: 130 | 44.1 | 0.85 | $C_{96}$ | $C_2$: 157 | 64.3 | 0.62 | $C_{98}$ | $C_2$: 174 | 41.9 | 0.87 |
| $C_{90}$ | $C_2$: 41 | 42.2 | 0.31 | $C_{92}$ | $C_2$: 64 | 39.7 | 0.56 | $C_{94}$ | $C_1$: 132 | 50.4 | 0.47 | $C_{96}$ | $C_1$: 101 | 65.2 | 0.86 | $C_{98}$ | $C_1$: 175 | 42.1 | 0.65 |
| $C_{90}$ | $C_2$: 45 | 83.0 | 0.46 | $C_{92}$ | $C_2$: 77 | 43.7 | 0.88 | $C_{94}$ | $C_1$: 129 | 46.6 | 0.84 | $C_{96}$ | $C_2$: 167 | 65.8 | 0.91 | $C_{98}$ | $C_1$: 168 | 43.3 | 0.64 |
| $C_{90}$ | $C_2$: 10 | 92.8 | 0.19 | $C_{92}$ | $C_2$: 36 | 50.5 | 0.58 | $C_{94}$ | $C_1$: 115 | 47.3 | 0.59 | $C_{96}$ | $C_1$: 159 | 67.6 | 0.84 | $C_{98}$ | $C_2$: 221 | 47.9 | 0.57 |
| $C_{90}$ | $C_2$: 23 | 81.3 | 0.50 | $C_{92}$ | $C_1$: 44 | 51.5 | 0.69 | $C_{94}$ | $C_1$: 125 | 49.7 | 0.62 | $C_{96}$ | $D_2$: 183 | 68.1 | 0.75 | $C_{98}$ | $C_2$: 246 | 48.5 | 0.81 |
| $C_{90}$ | $C_2$: 40 | 79.0 | 0.27 | $C_{92}$ | $C_2$: 61 | 56.5 | 0.89 | $C_{94}$ | $C_1$: 54 | 46.7 | 0.41 | $C_{96}$ | $C_1$: 160 | 80.1 | 0.46 | $C_{98}$ | $C_{2v}$: 167 | 48.6 | 0.56 |
| $C_{90}$ | $C_s$: 35 | 105.5 | 0.45 | $C_{92}$ | $C_s$: 16 | 61.2 | 0.35 | $C_{94}$ | $C_1$: 119 | 57.2 | 0.72 | $C_{96}$ | $C_2$: 55 | 94.7 | 0.64 | $C_{98}$ | $C_1$: 161 | 51.8 | 0.86 |
| | | | | | | | | | $Y_3N@C_{2n}$ | | | | | | | | | | |
| $C_{90}$ | $C_2$: 43 | 8.0 | 0.64 | $C_{92}$ | $D_3$: 85 | 0.0 | 0.82 | $C_{94}$ | $C_2$: 121 | 0.0 | 1.03 | $C_{96}$ | $D_2$: 186 | 0.0 | 0.97 | $C_{98}$ | $C_2$: 166 | 0.0 | 0.98 |
| $C_{90}$ | $C_2$: 44 | 0.0 | 0.97 | $C_{92}$ | $T$: 86 | 60.3 | 1.34 | $C_{94}$ | $C_2$: 126 | 28.6 | 0.87 | $C_{96}$ | $C_2$: 158 | 26.5 | 0.89 | $C_{98}$ | $C_1$: 247 | 33.4 | 0.73 |
| | | | | $C_{92}$ | $C_1$: 66 | 40.0 | 0.76 | | | | | $C_{96}$ | $D_{6d}$: 187 | 87.6 | 1.07 | $C_{98}$ | $C_2$: 252 | 27.7 | 0.81 |
| | | | | $C_{92}$ | $C_2$: 65 | 68.0 | 0.93 | | | | | | | | | | | | |

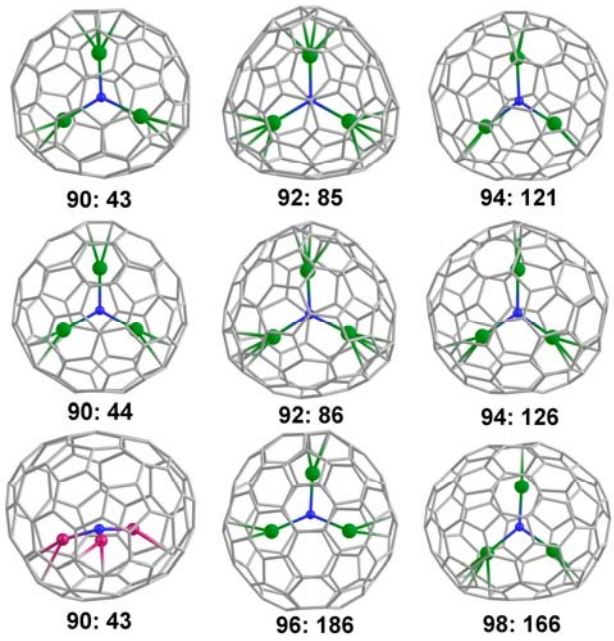


**Figure 3.** Molecular structures of selected $Y_3N@C_{2n}$ isomers with $2n$ = 90–98 (C – gray, N – blue, Sc – pink, Y – green). $Sc_3N@C_{90}$ ($C_2$: 43) is also shown for comparison. Y–C distances shorter than 2.580 Å and Sc–C distances shorter than 2.350 Å are shown as bonds.

while the isomer $C_{2v}$: 63751 is by 3.7 kJ/mol lower in energy. However, the latter has a small HOMO-LUMO gap (0.56 eV) and hence it is expected to be kinetically unstable. On the contrary, the isomer $Y_3N@C_{86}$ ($D_3$: 63761) has a gap of 1.47 eV and should thus be both thermodynamically and kinetically stable. This finding agrees well with X-ray crystallographic studies of $Tb_3N@C_{86}$, which was proved to have a $D_3$: 63761 cage.[23] The same cage structure may be suggested for $Tm_3N@C_{86}$[13] and $Dy_3N@C_{86}$.[21]

**$M_3N@C_{88}$.** The most stable isomer of $C_{88}^{6-}$, the IPR $D_2$: 81738 cage, is separated from all other structures by a gap of 70.6 kJ/mol. Hence, this isomer appears to be the most stable for $Sc_3N@C_{88}$ and $Y_3N@C_{88}$ (Fig. 2). The most stable non-IPR cage, $C_1$: 80982, is by 96.8, 57.2, and 78.3 kJ/mol less stable for $C_{88}^{6-}$, $Sc_3N@C_{88}$ and $Y_3N@C_{88}$, respectively. The HOMO-LUMO gap of 0.99 eV calculated for $Y_3N@C_{88}$ ($D_2$: 81738) suggests that this clusterfullerene might be kinetically stable. The thermodynamic and kinetic stability predicted for $Y_3N@C_{88}$ ($D_2$: 81738) agrees well with the result of X-ray crystallographic studies of $Tb_3N@C_{88}$, which is shown to have $D_2$: 81738 cage isomer.[23]

**$M_3N@C_{2n}$ ($2n$ = 90–98).** The studies of the $C_{82}^{6-}$–$C_{88}^{6-}$ isomers have shown that the relative stability of non-IPR isomers diminishes in comparison to the IPR structures with the increase of the cage size. This is manifested in the decrease of the number of non-IPR isomers present in the list of the ten most stable isomers, and also in the increase of the relative energy of the most stable non-IPR isomers with respect to the most stable IPR isomers (see Discussion section below). We suggest that this trend is valid for the larger fullerenes as well, and hence calculations of the $C_{90}^{6-}$–$C_{98}^{6-}$ fullerenes were performed only for IPR cages. Besides, computations for $Y_3N@C_{2n}$ ($2n$ = 90–98) isomers were limited to the cages with the highest stability and/or the largest HOMO-LUMO gap. Calculations for $Sc_3N@C_{2n}$ ($2n$ = 90–98) have no practical purposes as these clusterfullerenes have never been observed experimentally and besides, the results for the $C_{2n}$ ($2n \geq 82$) show that $Sc_3N$ cannot effectively interact with larger cages. However, for the sake of comparison and discussion of the general trends (see below), we performed DFT optimization for the $Sc_3N@C_{2n}$ isomers corresponding to the most stable $Y_3N@C_{2n}$ structures.

The two lowest energy isomers of $C_{90}^{6-}$, $C_2$: 43 and $C_2$: 44, have the largest HOMO-LUMO gaps (0.83 and 0.81 eV, respectively) among the ten most stable isomers and are shown to be almost isoenergetic ($C_2$: 44 is less stable by 13.5 kJ/mol). For $Y_3N@C_{90}$, the isomer $C_2$: 44 (Fig. 3) is 8.0 kJ/mol more stable and, more importantly, has a considerably larger HOMO-LUMO gap than the $C_2$: 43 isomer (0.97 eV *versus* 0.64 eV, respectively). Hence, $C_2$: 44 is suggested as the most probable cage isomer for the experimentally observed $Dy_3N@C_{90}$.[21]

The most stable isomer of $C_{92}^{6-}$ is $D_3$: 85, but this structure has a rather small HOMO-LUMO gap (0.63 eV), and the three following higher energy isomers with higher HOMO-LUMO gaps, $C_1$: 66 ($\Delta E$ = 22.3 kJ/mol, gap 0.81 eV), $T$: 86 ($\Delta E$ = 24.2 kJ/mol, gap 1.47 eV), and $C_2$: 65 ($\Delta E$ = 28.6 kJ/mol, gap 1.06 eV) may be also suggested as probable hosts for $M_3N$ clusters. For $Y_3N@C_{92}$, the isomer $D_3$: 85 (Fig. 3) is significantly stabilized compared the other structures, being at least by 60 kJ/mol lower in energy than the others. Hence, the $D_3$: 85 cage can be suggested for the experimentally observed $Dy_3N@C_{92}$,[21] but the other isomers ($C_1$: 66, $C_2$: 65, and especially $T$: 86) cannot be excluded because of the small HOMO-LUMO gap of $D_3$: 85, which may result in its low kinetic stability.

The most stable isomer of $C_{94}^{6-}$ is $C_2$: 121, and this structure also has the largest HOMO-LUMO gap (1.18 eV) among the ten lowest energy isomers. Calculations for $Y_3N@C_{94}$ were performed only for this structure and for the $C_2$: 126 isomer, which is the third most stable isomer ($\Delta E$ = 36.4 kJ/mol) and has a comparably large HOMO-LUMO gap (0.93 eV). $Y_3N@C_{94}$ ($C_2$: 121) (Fig. 3) is found to be by 28.6 kJ/mol more stable than the isomer based on the $C_2$: 126 cage, and the HOMO-LUMO gap of the former, 1.03 eV, suggest that this structure most probably corresponds to the experimentally observed $Dy_3N@C_{94}$.[21]

The most stable isomer of $C_{96}^{6-}$ is $D_2$: 186 (gap 1.06 eV) followed by $C_2$: 158 ($\Delta E$ = 28.0, gap 0.88 eV) and $D_{6d}$: 187 ($\Delta E$ = 54.2 kJ/mol, gap = 1.50 eV). Only these three structures were further considered for $Y_3N@C_{96}$ as other isomers are less stable and have small HOMO-LUMO gaps (less than 1 eV). It is found that $Y_3N@C_{96}$ ($D_2$: 186) (Fig. 3) is the lowest energy isomer as in the case of empty cages, and its HOMO-LUMO gap (0.97 eV) is rather close to that of $C_{96}^{6-}$. The larger gap, 1.07 eV, is

predicted for $Y_3N@C_{96}$ ($D_{6d}$: 187), but this isomer is less thermodynamically stable ($\Delta E$ = 87.6 kJ/mol). Moreover, a significant decrease of the gap after encapsulation of the $Y_3N$ cluster points to the ineffective cluster-cage interactions in this cage. Finally, $Y_3N@C_{96}$ ($C_2$: 158) is less stable than $D_2$: 186 by 26.6 kJ/mol and has a small HOMO-LUMO gap (0.59 eV). Thus, the experimentally observed $Dy_3N@C_{96}$[21] most probably has the $D_2$: 186 cage structure.

The lowest energy isomer of $C_{98}^{6-}$ is $C_2$: 166, and this structure also has the largest HOMO-LUMO gap among the ten most stable isomers of $C_{98}^{6-}$. Thus, calculations for $Y_3N@C_{98}$ isomers were performed for $C_2$: 166 (Fig. 3) and also for second and the third most stable isomers of $C_{98}^{6-}$, $C_1$: 247 ($\Delta E$ = 16.1 kJ/mol, gap 0.99 eV) and $C_2$: 252 ($\Delta E$ = 29.8 kJ/mol, gap 0.97 eV). The higher energy isomers of $C_{98}^{6-}$ have smaller HOMO-LUMO gaps (less than 0.87 eV) and were not considered for $Y_3N@C_{98}$. The isomer $C_2$: 166 is also the most stable for $Y_3N@C_{98}$, and has HOMO-LUMO gap of 0.98 eV. Cluster-cage interactions in the $C_1$: 247 and $C_2$: 252 isomers are less effective, which results in their lower thermodynamic stability and significant decrease if the HOMO-LUMO gap as compared to the empty cages. Thus, $C_2$: 166 is considered to be the most probable cage isomer of $Dy_3N@C_{98}$.[21]

## Discussion

**Correlation of calculated values with the experimental data and assignment of new cages.** The methodology adopted in this work – i.e. prescreening of thousands of $C_{2n}^{6-}$ isomers at the AM1 level followed by DFT calculations of the lowest energy cages – enabled us to determine the most stable isomers of $Sc_3N@C_{2n}$ and $Y_3N@C_{2n}$ in a wide range of cage sizes. More importantly, it appears that the most stable isomers found in this work are those which were confirmed experimentally, at least for $Sc_3N@C_{68}$,[6] $Sc_3N@C_{78}$,[7] $M_3N@C_{80}$ ($I_h$),[24, 25, 47] $M_3N@C_{80}$ ($D_{5h}$),[10, 23] $Tb_3N@C_{84}$,[22] $Tb_3N@C_{86}$,[23] and $Tb_3N@C_{88}$,[23] characterized by single-crystal X-ray diffraction, and for $Sc_3N@C_{70}$ and $M_3N@C_{78}$, which structures are elucidated based on the DFT calculations and vibrational spectroscopy.[11, 39] If there are two or more isomers of the same composition ($M_3N@C_{80}$, $M_3N@C_{78}$, $M_3N@C_{84}$), the most abundant structures were predicted in this work to be more stable. It should be emphasized that our

results are obtained from the first principles, without the use of any preliminary information such as cage symmetry. The only assumption used was that three or more adjacent pentagons in the fullerene cage could be avoided. On the one hand, our findings confirm the reliability of the PBE/TZ2P method for the prediction of the relative stabilities of nitride clusterfullerenes. On the other hand, though the conditions at which fullerenes are formed can hardly be described by a chemical equilibrium, our results demonstrate that the products are preferably formed under thermodynamic stability control. Hence, in the absence of unambiguous structural information on the nitride clusterfullerenes from experimental studies, the determination of the most stable isomers by DFT computations may be considered as a reasonable and reliable alternative to the X-ray crystallographic studies, especially if supported by spectroscopic information such as optical band-gap and vibrational spectra. Specifically, results of this work may be used for a tentative structural assignment for those structures, which cannot be characterized by X-ray diffraction at this time.

As the calculations are performed under the assumption that the stability of $M_3N@C_{2n}$ correlates with that of $C_{2n}^{6-}$, these results can be used for the assignment of the cage isomers of $M_2@C_{2n}$ endohedral fullerenes, where M is a trivalent metal. Moreover, even a better correlation between the stability of $C_{2n}^{6-}$ and $M_2@C_{2n}$ is expected because such a factor like the cage dimensions (see discussion below), which can be definitive for $M_3N@C_{2n}$ isomers, cannot play an important role for dimetallofullerenes. For instance, $La_2@C_{72}$ is known to have $D_2$ symmetry from the $^{13}C$ NMR spectra,[30] and recently Slanina *et al.*[48] performed series of DFT calculations for isomers of $C_{72}^{6-}$ with $D_2$ or higher symmetry and found that the most stable isomer is based on cage $D_2$: 10611. Our calculations of the $C_{72}$ hexaanions (Table 2), which were not limited to $D_2$ isomers, also predict this isomer to be the most stable one.

$Sc_2@C_{76}$ isolated by Wang et al.[49] was found to have 35 $^{13}C$ NMR lines, three of which had double intensity. Considering only IPR isomers, it was supposed that the molecule was based on $D_2$: 19150 isomer, and lower symmetry determined by NMR spectroscopy was due to the presence of two isomers with the same carbon cage but different position of Sc atoms. The results of this work show that $D_2$: 19150 is unstable in the hexaanionic state, and the formation of $Sc_2@C_{76}$ based on $C_s$: 17490 cage might

be expected. Though this isomer should produce a somewhat different $^{13}C$ NMR pattern (6 single intensity and 35 double intensity peaks), it cannot be excluded by experimental data because of a low signal-to-noise ratio and the coincidence of some peaks. To validate this assignment we have performed calculations for a series of $Sc_2@C_{76}$ isomers based on $C_s$: 17490, $C_2$: 17765, $C_2$: 17765, $C_2$: 17512, $C_2$: 18161, and $D_2$: 19150 cages, chosen from the lowest energy $C_{76}^{6-}$ isomers because of their compatibility with the $^{13}C$ NMR data. The relative energies are listed in Table 5. $Sc_2@C_{76}$ ($C_s$: 17490) (Fig. 4) is indeed the lowest energy isomer, being by 50–90 kJ/mol more stable than the other $C_2$-symmetric structures, while the $D_2$: 19150 isomer is at least by 141 kJ/mol less stable. Interestingly, the band-gap of $Sc_2@C_{76}$ ($C_s$: 17490) is only 0.72 eV, which is by 0.40 eV smaller than the value of 1.12 eV predicted for $Sc_3N@C_{76}$ ($C_s$: 17490). Smaller band-gaps were also observed for $La_2@C_{78}$[50] (ca 1.00 eV based on the onset value) and $La_2@C_{80}$[12] (1.41 eV) as opposed to $Sc_3N@C_{78}$[34] (1.41 eV) and $Sc_3N@C_{80}$[12] (1.69 eV), though these endohedral fullerenes are based on the same cage isomers of $C_{78}$ and $C_{80}$, respectively. The DFT predicted value agrees well with the optical band-gap of 0.94 eV determined in the experimental absorption spectrum of $Sc_2@C_{76}$ (note that the method used systematically underestimates band-gaps of endohedral fullerenes by ca 0.2–0.3 eV). Thus, the reassignment of $Sc_2@C_{76}$ to the non-IPR $C_s$: 17490 cage is proposed as a result of this work.

**Stability of the cage isomers on the per-atomic basis**. The broad range of the fullerene sizes studied in this work enabled us to follow the general trends in their stabilities. To compare the energies of the fullerenes of different size, the absolute energies were normalized to the number of atoms in the given fullerene. Figure 5 plots the normalized energies of the most stable $C_{2n}^{6-}$ isomers versus the number of atoms. The smooth decrease of the energy is observed, which can be perfectly fitted by an exponential decay (Fig. 5). This trend can be explained by a reinforcing combination of two factors: (i) the decrease of the curvature of the cage with the increase of the cage size, which decreases the strain and hence increases the stability on the per-atomic basis, and (ii) the increase of the cage size decreases the on-site Coulomb repulsions of six surplus electrons in $C_{2n}^{6-}$. However, deviations of 0.013 and 0.024 eV from the exponential function for $C_{80}$ ($I_h$: 31924) and $C_{80}$ ($D_{5h}$: 31923) isomers are obvious; in other words,

***Table 5.*** Relative energies (Δ*E*, kJ/mol), and HOMO-LUMO gaps (gap, eV) for selected $Sc_2@C_{76}$ isomers as computed at the DFT level.

| Cage | $C_{76}^{6-}$ | | $Sc_2@C_{76}$ | |
|---|---|---|---|---|
| isomer | Δ*E* | gap | Δ*E* | gap |
| $C_s$: 17490 | 0.0 | 1.12 | 0.0 | 0.72 |
| $C_2$: 17765 | 55.8 | 1.37 | 74.7 | 0.79 |
| $C_2$: 17512 | 60.1 | 1.14 | 51.2 | 0.91 |
| $C_2$: 18161 | 64.7 | 1.12 | 88.6 | 0.51 |
| $D_2$: 19150 | 101.0 | 0.75 | 122.8 | 0.65 |

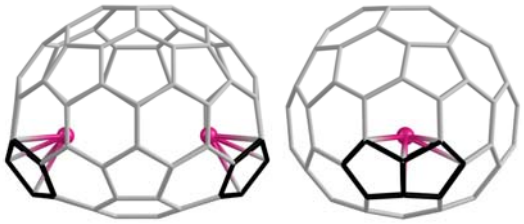

**Figure 4.** Molecular structure of the lowest energy isomer of $Sc_2@C_{76}$ ($C_s$: 17490). Adjacent pentagons are highlighted in black, Sc–C distances shorter than 2.350 Å are shown as bonds. DFT-optimized Sc–Sc distance in this structure is 4.876 Å. Hessian calculations confirmed that this structure is the energy minimum (i.e. it has no imaginary frequencies).

these isomers are by 98 and 185 kJ/mol more stable than they might be if they were like all other fullerenes (those which obey the smooth decay in the normalized energy). The enhanced stability of the two $C_{80}^{6-}$ isomers explains the increased yield of $M_3N@C_{80}$ compared to all other cage sizes (for instance, $Dy_3N@C_{80}$ ($I_h$: 31924) and $Dy_3N@C_{80}$ ($D_{5h}$: 31923) constitute ca 70 and 10 mol. %, respectively, of the whole $Dy_3N@C_{2n}$ mixture obtained in the synthesis).[21] $Sc_3N@C_{72}$ and $Sc_3N@C_{74}$ may be used as an example of the opposite situation: the cages, which correspond to the most stable isomers of these clusterfullerenes, are relatively unstable in the $C_{2n}^{6-}$ form (77.3 and 86.9 kJ/mol, respectively, above the isomers which normalized energy lies on the line in Fig. 5), and this might be one of the reasons why $Sc_3N@C_{72}$ and $Sc_3N@C_{74}$ are not formed in the arc burning in noticeable amounts.

Thus, not only the isomeric structure of the clusterfullerenes correlates with the DFT-predicted relative stability of the isomers, but also the experimental yields of $M_3N@C_{2n}$ correlate with the stability of $C_{2n}^{6-}$ cage on per-atomic basis. The cage should be stable enough to favor the formation of the clusterfullerenes, and if its normalized energy is significantly higher than the fitting curve in Fig. 5, clusterfullerenes may not be formed at all.

**Isolated Pentagon Rule and Cage Size.** The specific feature of the $M_3N@C_{2n}$ fullerenes and the $C_{2n}^{6-}$ hexaanions is that the non-IPR isomers can compete in stability with the IPR structures, and in many cases non-IPR fullerenes are even more stable than the IPR ones (see Tables 2–4). In fact, a fairly systematic correlation between the relative stability of non-IR isomers and the cage size can be found. Figure 6 plots the number of IPR isomers and the isomers with one, two or three APPs among the ten lowest energy isomers of $C_{2n}^{6-}$ for each cage size *versus* the number of atoms in the fullerene (note, that there are no isomers with four or more APPs among the lowest energy structures for any cage size studied). It is obvious that for small fullerenes ($C_{68}$, $C_{70}$) the isomers with three APPs are dominating, but starting from $C_{76}^{6-}$ there are no such isomers among the most stable structures. The isomers with two APPs are dominating for $C_{72}^{6-}$ – $C_{78}^{6-}$, but not for larger cages. Finally, the highest number of isomers with one APP can be found for $C_{80}^{6-}$ – $C_{86}^{6-}$. Significantly, the number of IPR isomers among

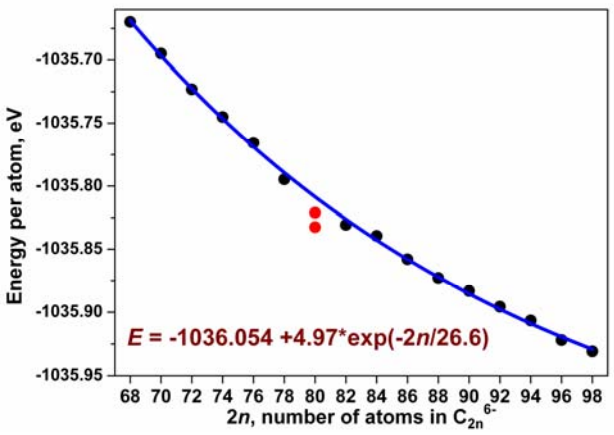


**Figure 5.** Normalized energies of the most stable $C_{2n}^{6-}$ isomers (black dots) and their fit with the exponential decay function (blue line). Normalized energies for $C_{80}^{6-}$ $I_h$: 31924 and $D_{5h}$: 31923 isomers are shown as red dots.

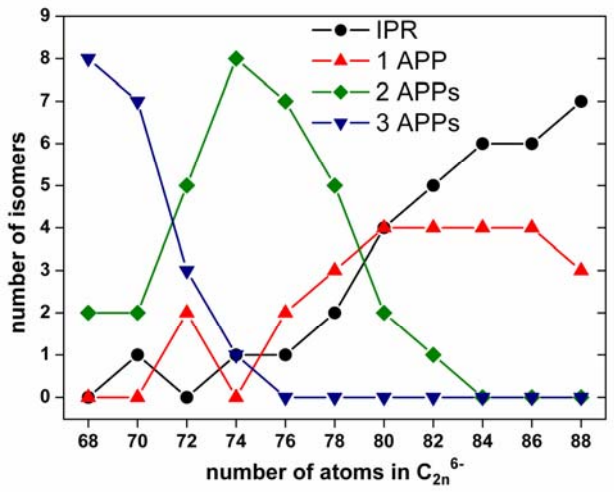


**Figure 6.** The number of isomers with given number of APPs among the ten lowest energy $C_{2n}^{6-}$ isomers plotted as a function of 2*n*. The total numbers of IPR isomers available for $C_{68}$–$C_{88}$ are listed in Table 1.

the lowest energy structures is increasing with the cage size. Moreover, the relative energies of the most stable IPR and non-IPR isomers also follow a similar trend – the non-IPR isomers become less and less stable as the fullerene size increases (see Tables 2–4), and starting from $C_{86}^{6-}$ the non-IPR isomers cannot compete in stability with the IPR ones (this is also true for $C_{80}^{6-}$, but in this case it happens because of unusually high stability of $I_h$: 31924 and $D_{5h}$: 31923 isomers). Hence, the formation of non-IPR endohedral fullerenes for larger cages is highly unlikely.

It should be noted that the isolated pentagon rule, which disfavours fullerene isomers with edge-sharing pentagons due to an increased local strain for the carbon atoms on the pentagon-pentagon edges, is justified for the uncharged carbon cages with the amount of π-electrons coinciding with the amount of carbon atoms.[46] The result of the six-fold electron transfer to the fullerene may be formally conceived as a change of the hybridization state of six carbon atoms from $sp^2$ to $sp^3$ (of course, it should not be taken literally because the charge is often delocalized over the cage, but still this assumption appears to be instructive). As the pentagon adjacencies may be stabilized by the change of the hybridization of the carbon atoms in pentagon/pentagon junctions to C($sp^3$) state, which can be exemplified by the isolation of the stable $C_{50}Cl_{10}$[51] or $C_{64}H_4$[52] non-IPR fullerenes, one may conceive that the six-fold electron transfer to the fullerene can stabilize up to three APPs. This reasoning agrees with the fact that the $C_{2n}^{6-}$ isomers with more than three APPs were not found among the lowest energy structures. However, the influence of the 6-fold charging of the fullerene should be diminished with the growth of the cage size and hence its stabilizing role for the pentagon adjacencies is leveled down for larger fullerenes. With the increase of the cage size a more uniform distribution of the pentagon-induced strain over the fullerene is possible and hence, localization of such a strain in pentagon adjacencies should become more unfavorable than for the smaller cages.

**Stability of IPR isomers.** The exclusive stability of the $I_h$: 31924 and $D_{5h}$: 31923 isomers of $C_{80}^{6-}$ discussed above may be understood recalling their hexagon indices, defined by Raghavachari[53] to quantify the distribution of pentagon-induced curvature in IPR fullerenes. According to the definition, the neighbor index of each hexagon is the number of hexagons to which it is adjacent, and every

fullerene isomer can be characterized by a set of indices ($h_0$, $h_1$, $h_2$, $h_3$, $h_4$, $h_5$, $h_6$), where $h_k$ is the number of hexagons with neighbor index $k$. As each hexagon in the IPR isomer is adjacent to at least three other hexagons, $h_0$, $h_1$, and $h_2$ are equal to 0 for all IPR isomers, and the combination of only four indices ($h_3$, $h_4$, $h_5$, $h_6$) may be used as a signature of hexagon adjacencies in a given fullerene isomer.[46, 53] According to Raghavachari,[53] the indices of all hexagons should be as close to each other as possible to minimize the steric strain. Hence, the lowest strain is expected for those structures, in which all indices are equal, and for the range of cage sizes studied in the work, $C_{68}$–$C_{98}$, this condition is fulfilled only for $C_{80}$ ($I_h$: 31924) and $C_{80}$ ($D_{5h}$: 31923), the index combination of which is (0, 30, 0, 0).[46] Thus, the exceptional stability of these $C_{80}^{6-}$ isomers may be explained by the favorable distribution of the pentagons, which leads to the least steric strain. More complex conditions had to be derived for other IPR fullerenes, namely, ($h_3$, $h_4$, $h_5$, $h_6$) indices should be ($80 - 2n$, $3n - 90$, 0, 0) for $C_{2n}$ with $2n \leq 80$, and (0, $70 - n$, $2n - 80$, 0) for $C_{2n}$ with $2n \geq 80$.[46] For the IPR isomers of $C_{76}$–$C_{88}$ these conditions are satisfied for $C_{76}$ ($T_d$: 19151), $C_{78}$ ($D_{3h}$: 24109), $C_{82}$ ($C_{2v}$: 39718), $C_{84}$ ($D_2$: 51589), $C_{84}$ ($D_2$: 51590), $C_{84}$ ($D_{2d}$: 51591), $C_{86}$ ($D_3$: 63761), and $C_{88}$ ($D_2$: 81738). This list perfectly corresponds to the lowest energy IPR isomers of $C_{76}^{6-}$–$C_{88}^{6-}$ found in this work. For larger cages these conditions are less instructive, because many of the IPR isomers satisfy them, but still one can notice that the lowest energy isomers of $C_{90}^{6-}$–$C_{98}^{6-}$ also have the optimum distribution of pentagons. Interestingly, it appears that the relative energies of the IPR $C_{2n}^{6-}$ isomers follow the rationalization of the stability based on the steric strain much better than the relative energies of uncharged fullerenes. DFT calculations predict that, by violation of the above specified conditions, the most stable uncharged IPR isomers are $D_2$: 19150 for $C_{76}$,[54] $D_{5d}$: 31918 for $C_{80}$,[54, 55] $C_2$: 39712 for $C_{82}$,[54, 56] $C_2$: 63759 for $C_{86}$,[54] and $C_s$: 17 for $C_{88}$.[57]

**Structural Relationships Between The Fullerenes**. Analysis of the cage structures of the lowest energy $M_3N@C_{2n}$ isomers revealed that many of them have common structural motifs, and we could find two groups of interrelated structures. The first group consists of the $C_{70}$ ($C_{2v}$: 7854), $C_{72}$ ($C_s$: 10528), and $C_{74}$ ($C_{2v}$: 14239) cages, all corresponding to the most stable $Sc_3N@C_{2n}$ isomers. The structure of $C_{72}$ ($C_s$: 10528) can be envisaged as a result of addition of two carbon atoms to $C_{70}$ ($C_{2v}$:

7854) near to one of its APPs with small structural rearrangements of the whole structure (see Fig. S1 in supporting information). Likewise, $C_{74}$ ($C_{2v}$: 14239) can be obtained after the addition of two carbon atoms to $C_{72}$ ($C_s$: 10528) near to the place, where the atoms were added to $C_{70}$ ($C_{2v}$: 7854) to form $C_{72}$ ($C_s$: 10528). Thus, the major part of the cage is the same for all three structures.

The second group comprises $C_{76}$ ($C_s$: 17490), $C_{78}$ ($C_2$: 22010), $C_{82}$ ($C_{2v}$: 39705), and $C_{84}$ ($C_s$: 51365). These cages correspond to the lowest energy isomers of $Y_3N@C_{2n}$ and all of them are structurally related to $C_{80}$ ($I_h$: 31924). Figure 7 shows Schlegel diagrams of these cages demonstrating how they can be obtained by removal or addition of certain atoms and bonds in $C_{80}$ ($I_h$: 31924). For instance, $C_{82}$ ($C_{2v}$: 39705) can be obtained from $C_{80}$ ($I_h$: 31924) by insertion of a $C_2$ unit into the center of a hexagon. In general, it can be seen that aside from the local transformations, all these cages share the common motif of $C_{80}$ ($I_h$: 31924). Finally, $C_{82}$ ($C_s$: 39663), which is also considered as a possible structure for $M_3N@C_{82}$, is closely related to $C_{84}$ ($C_s$: 51365) and can be obtained from the latter by the removal of two carbon atoms with subsequent pairwise Stone-Wales transformation (see Fig. S2a). On the other hand, this cage can be obtained form the $C_{78}$ ($D_{3h}$: 24109) by the insertion of four carbon atoms in the local fragment of the latter (Fig. S2b).

The structural relationships between the cage isomers, especially in the second group, demonstrate that the high stability of these particular cage isomers is not accidental. We have already pointed out that the exceptional stability of $C_{80}^{6-}$ ($I_h$: 31924) can be explained by the special distribution of the pentagons, which minimizes the strain of the cage. Certainly, this factor remains important for other fullerenes, even though they may be non-IPR, and in this regard the high stability of the cages retaining significant part of the $C_{80}$ ($I_h$: 31924) cage is not surprising. Moreover, the exceptional stability of $C_{80}^{6-}$ ($I_h$: 31924) on the per-atomic basis appears to be one of the reasons why non-IPR isomers retaining significant part of its structure can compete in stability with IPR isomers.

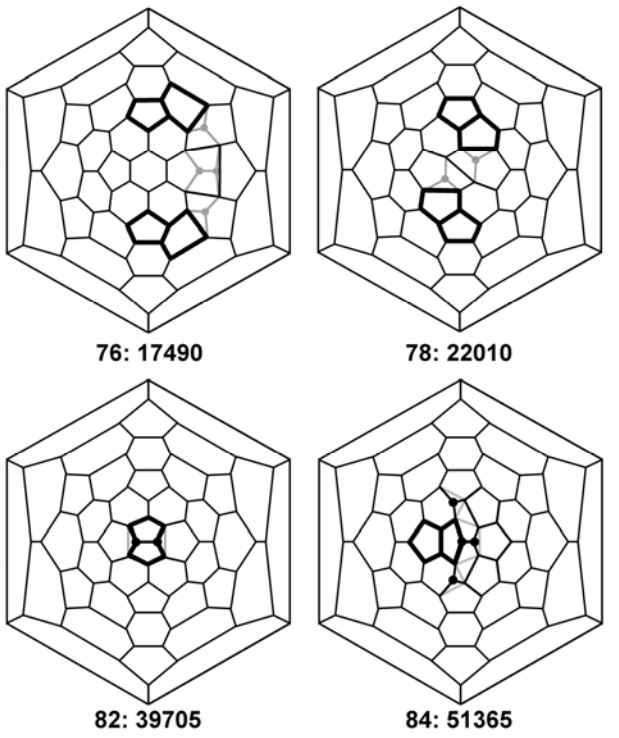


**Figure 7.** Schlegel diagrams of $C_{76}$ ($C_s$: 17490), $C_{78}$ ($C_s$: 22010), $C_{82}$ ($C_{2v}$; 39705), and $C_{84}$ ($C_s$: 51365) showing the relationships of these structures to $C_{80}$ ($I_h$: 31924). The atoms and bonds in $C_{80}$, which should be removed, are shown as gray circles and lines, respectively. The atoms, which should be added to $C_{80}$ to obtain $C_{82}$ and $C_{84}$, are shown as black circles. APPs are shown in thick black lines.

**Cluster-Cage Interactions.** The data in tables 2–4 demonstrate that though the cage stability is very important in determining the structures of clusterfullerenes, the trends in the relative energies of $M_3N@C_{2n}$ isomers cannot be explained by this factor alone. Obviously, the cage should provide a suitable geometry for the enclosed cluster, that is, there should be enough inner space in the cage for the latter. The most striking example of the influence of this factor is the case of $M_3N@C_{78}$, in which an insufficient cage size of the $D_{3h}$: 24109 isomer for the $Y_3N$ cluster results in the formation of different cage isomers of $Sc_3N@C_{78}$ and $M_3N@C_{78}$ (M = Dy, Tm) clusterfullerenes.[39] Besides, if the fullerene has APPs, they should be located in such a way that their coordination by Sc atoms of the cluster is possible without a significant distortion of the latter. When this condition is not fulfilled for the lowest energy $C_{2n}^{6-}$ isomers, the $M_3N@C_{2n}$ isomers of these cages are destabilized and the most stable isomers of the clusterfullerenes are based on the relatively unstable cages. As a result, such clusterfullerenes might be absent in the products of the arc-discharge synthesis at all, as can be exemplified by $Sc_3N@C_{72}$ and $Sc_3N@C_{74}$, for which the lowest energy isomers of $C_{2n}^{6-}$ have unfavorable arrangement of APPs.

To quantify the influence of the cage geometry on the cluster-cage interaction we have analyzed the cluster binding energy (BE) in the series of $M_3N@C_{2n}$ clusterfullerenes, which are listed in Table S1. The binding energy of the cluster may be defined as the energy change in the reaction $M_3N + C_{2n} = M_3N@C_{2n}$, which will be further referred to as BE-1. Table S1 (Supporting Information) lists BE-1 values computed in this work for a series of $Sc_3N@C_{2n}$ and $Y_3N@C_{2n}$ clusterfullerenes.

Earlier, BE-1 values for experimentally isolated $Sc_3N@C_{2n}$ clusterfullerenes were reported to be –12.07 eV for $Sc_3N@C_{68}$ at the B3LYP/6-31G* level;[58] –9.73 and –9.62 eV for $Sc_3N@C_{78}$ at the BP/TZP[33, 59] and B3LYP/6-31G* levels,[58] respectively; –10.72 and –11.60 eV for $Sc_3N@C_{80}$ at the BLYP//B3LYP/6-31G*[60] and BP/TZP levels,[33] respectively. The values computed in this work, –12.50, –10.51, and –12.48 eV for $Sc_3N@C_{68}$ ($D_3$: 6140), $Sc_3N@C_{78}$ ($D_{3h}$: 24109) and $Sc_3N@C_{80}$ ($I_h$: 31934) respectively, are by 0.5 – 0.8 eV larger, but the same trend in the values is observed (almost identical values for $Sc_3N@C_{68}$ and $Sc_3N@C_{80}$ and smaller BE-1 value for $Sc_3N@C_{78}$). The values predicted for

$Sc_3N@C_{70}$ ($C_{2v}$: 7854), –12.43 eV, and $Sc_3N@C_{80}$ ($D_{5h}$: 31923), –12.38 eV, are also close to the BE-1 values of $Sc_3N@C_{68}$ and $Sc_3N@C_{80}$ ($I_h$: 31924). In fact, the values for four of the five experimentally isolated $Sc_3N@C_{2n}$ clusterfullerenes are the highest among the whole series of $Sc_3N@C_{2n}$ molecules studied theoretically in this work.

The BE-1 values for $Y_3N@C_{2n}$ with small cages ($2n < 78$) are all below 10 eV (Table S1). The largest value, –11.32 eV, is predicted for $Y_3N@C_{84}$ ($C_s$: 51365), which has the same cage isomer as the experimentally isolated $Tb_3N@C_{84}$. Comparably large BE-1 values are also predicted for $Y_3N@C_{2n}$ with other experimentally observed cage isomers: –10.82 eV for $Y_3N@C_{78}$ ($C_2$: 22010), –10.38 eV for $Y_3N@C_{80}$ ($I_h$: 31924), –10.25 eV for $Y_3N@C_{80}$ ($D_{5h}$: 31923), –10.37 eV for $Y_3N@C_{88}$ ($D_2$: 81738). Finally, similar values are also predicted for some of the structures suggested in this study for the clusterfullerenes, which are not yet structurally characterized: –10.98 eV for $Y_3N@C_{82}$ ($C_{2v}$: 39705), –10.35 eV in $Y_3N@C_{82}$ ($C_s$: 39663), –10.90 eV for $Y_3N@C_{92}$ ($D_3$: 85). Note that the largest BE-1 values for $Y_3N@C_{2n}$ are systematically smaller than the largest values for $Sc_3N@C_{2n}$.

Though experimentally isolated $M_3N@C_{2n}$ structures usually have large BE-1 values, some of them do not: the opposite examples are $Sc_3N@C_{78}$ ($D_{3h}$: 24109) and $Y_3N@C_{86}$ ($D_3$: 63761). On the other hand, some of the non-isolated compounds are also expected to have a large BE-1 (see Table S1). Hence, BE-1 values may be misleading in some cases and appear to be not very instructive for the goal of this study. Since the relative stability of the empty fullerene isomers is strongly affected by the charge, BE-1 values are determined not only by the effect of the cage geometry and cluster-cage interaction, but also by the relative stabilities of the cages in the neutral state. For instance, BE-1 for the non-IPR $C_2$: 22010 isomer of $Sc_3N@C_{78}$ is higher than that of the IPR $D_{3h}$: 24109 isomer because the non-IPR isomer is substantially less stable in the neutral form (by 234.0 kJ/mol), rather than because this non-IPR isomer is more suitable for the encapsulation of the $Sc_3N$ cluster. Likewise, the small BE-1 value for $Sc_3N@C_{78}$ in comparison to all other $Sc_3N$-based clusterfullerenes can be explained by the fact that $D_{3h}$: 24109 is the only stable cage in the uncharged form (it is predicted to be the second lowest energy IPR isomer of $C_{78}$[54]), while other cages found in $Sc_3N@C_{2n}$ are unstable in the uncharged form.

To focus presumably on the effect of the cage geometry and the cluster-cage bond formation on the BE, we have also computed the energy changes in the reaction $M_3N^{6+} + C_{2n}^{6-} = M_3N@C_{2n}$. The values computed this way (named BE-2 hereafter) should be less sensitive to the relative stability of the empty cages because the hexaanion is used as the starting state of the fullerene.[61] However, the drawback of this scheme is that the energy in this case is dominated by the large classical Coulomb term. For instance, 125.3 eV are released by placing the 6+ point charge into the center of the 6– charged sphere with the radius of 4.138 Å (i.e. the radius of DFT-optimized $I_h$: 31924 isomer of $C_{80}^{6-}$),[62] which is close to 123.9 and 133.2 eV, DFT-computed BE-2 values computed for $Y_3N@C_{80}$ ($I_h$: 31924) and $Sc_3N@C_{80}$ ($I_h$: 31924), respectively. Moreover, as the electrostatic potential inside the charged sphere scales with the sphere radius as $R^{-1}$, one may expect that the absolute BE-2 values should decrease smoothly with the increase of the cage size.

BE-2 values for all studied compounds are listed in Table S2 (Supporting Information). Fig. 8 plots the BE-2 values for the most stable $M_3N@C_{2n}$ isomers for each $2n$, and also the average values for a set of ten isomer with the lowest energy $C_{2n}^{6-}$ cages together with a 95% confidence interval *versus* the cage size.

It is shown that for the same cage isomer, the binding energies for $Y_3N$ are by 9 – 10 eV smaller than those for $Sc_3N$. The reason of this is not clear yet, but in fact it correlates with the lower yields of $Y_3N$ and lanthanide-based clusterfullerenes compared to $Sc_3N@C_{2n}$. The BE-2 becomes systematically smaller with the increase of the cage size, which can be explained by the classical Coulomb interaction as discussed above. When the 95% probability confidence interval may be estimated (for a set of data with ten points it is defined as 2.31 times standard deviation), its magnitude varies considerably with the cage size. For $Sc_3N@C_{2n}$, the magnitude is the largest for the smallest cage, $2n = 68$, then it decreases to the cage size of $2n = 76$, and remains almost the same for the higher cages. For $Y_3N@C_{2n}$, the largest magnitudes are found for $C_{78}$ and $C_{80}$, while for larger cages the interval decreases rapidly, remaining almost constant for $C_{86}$ and $C_{88}$. Thus, it appears that for large cage sizes

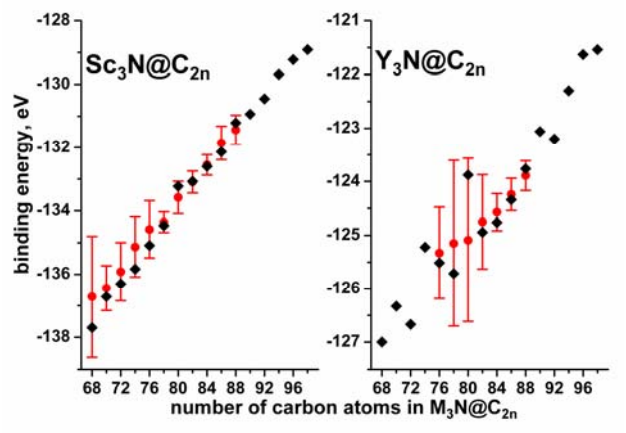


**Figure 8.** BE-2 values for the lowest energy isomers of $Sc_3N@C_{2n}$ and $Y_3N@C_{2n}$ (black squares) and mean BE-2 values for ten lowest energy isomers together with 95% probability confidence interval (red dots and "error" bars) plotted as the function of the number of atoms in the fullerenes

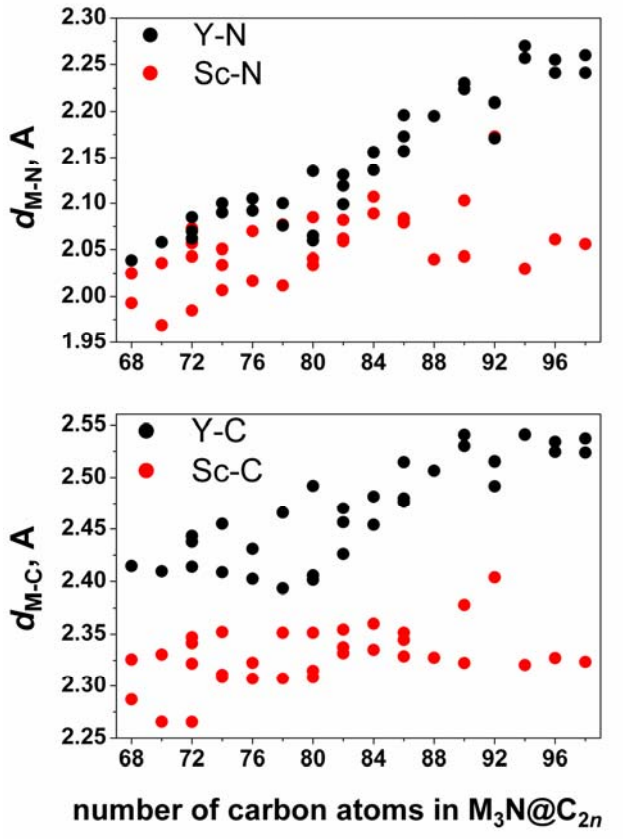


**Figure 9.** Averaged Sc–N, Y–N, Sc–C and Y–C distances in selected $Sc_3N@C_{2n}$ and $Y_3N@C_{2n}$ isomers listed in Table 6 (the isomers from Tables 4 are also added for $Y_3N@C_{2n}$, $2n$ = 90–98) plotted as a function of the cage size.

the range of BE-2 values is rather small, which means that for these cages the difference in their shape and dimensions are relatively unimportant for the cluster. On the contrary, this factor is very important for smaller cages. For $Sc_3N$, the shape of the cage is one of the definitive factors up to $Sc_3N@C_{76}$, while for larger $Y_3N$ cluster it is important up to $C_{82}$. Significantly, besides the size of the cage and the cluster, for $Sc_3N@C_{2n}$ clusterfullerenes with smaller cages the location of APPs is also very important because most of the cage isomers in the $C_{68}$–$C_{76}$ cage sizes have two–three APPs. It is obvious from the data presented above that the coordination of the metal atoms to APPs is important for stabilization of the latter, and hence only the cages which topology allows coordination of *all* APPs can lead to the stable $Sc_3N@C_{2n}$ isomers. This factor is less important for $Y_3N@C_{2n}$ clusterfullerenes because the size of $Y_3N$ cluster is simply too large to fit the cages smaller than $C_{76}$, while larger cages have smaller number of APPs.

Interestingly, BE-2 values for the most stable $M_3N@C_{2n}$ isomers are usually lower than or close to the average value for a set of ten isomers, with the exception of $M_3N@C_{80}$. It is obvious, that for $Y_3N@C_{80}$ ($I_h$: 31924) the encapsulation of the cluster is substantially less favorable than for most of the other $C_{80}$ isomers, because $Y_3N$ cluster is already too large for this almost spherical cage (similar conclusion was also reported by Gan et al.[63]). It is the only exclusive stability of the cage which makes $Y_3N@C_{80}$ ($I_h$: 31924) the lowest energy isomer.

**The optimum M–N and M–C distances.** To study the influence of the cage size and shape on the cluster geometry and metal–carbon distances, average Sc–N, Y–N, Sc–C, and Y–C interatomic distances in selected isomers of $Sc_3N@C_{2n}$ and $Y_3N@C_{2n}$ were studied (for Sc–C and Y–C, nine shortest M–C bonds were averaged). Figure 9 plots these distances versus the cage size of the isomers of $Sc_3N@C_{2n}$ and $Y_3N@C_{2n}$ listed in Table S1. Though the values for different isomers of the given cage size are significantly scattered, it is still possible to figure out that the longest Sc–N bond distances do not exceed 2.10 Å, and this maximum value does not depend on the cage size. On the contrary, the Y–N distances increase systematically with the cage size up to $C_{90}$, while for larger cages the saturation of the bondlengths around 2.25 Å is found. In a similar fashion, averaged Sc–C bonds for $Sc_3N@C_{74}$–

$Sc_3N@C_{98}$ stay in the narrow range of 2.30–2.35 Å, while Y–C distances show a tendency to increase up to ca 2.50–2.55 Å in $Y_3N@C_{90}$, and these values are preserved for large cages. The only exclusion from these rules is $M_3N@C_{92}$ ($D_3$: 85) with M being both Sc and Y, as Sc–N and Sc–C distances are much longer than in all other $Sc_3N@C_{2n}$ molecules, while Y–N and Y–C distances are, on the contrary, shorter than in other $Y_3N@C_{2n}$ molecules of similar cage size.

To understand why $M_3N@C_{92}$ ($D_3$: 85) shows different geometry parameters from all other clusterfullerenes we have analyzed the nature of bonding between the cluster and the cage in this and other clusterfullerenes. Interestingly, in $M_3N@C_{92}$ ($D_3$: 85) the metal atoms a coordinated to pyracelene units, and analysis of spatial distribution of MOs shows that some of them are largely localized on the pyracelene units and have large metal-carbon bonding contributions. Similar MOs were found in $Sc_3N@C_{78}$ ($D_{3h}$: 24109), in which Sc atoms are also bonded to the pyracelene units.[33,34] On the contrary, in most other clusterfullerenes it is difficult to point to the MOs with considerable metal-cage bonding contribution; instead, metal-cage covalent interactions are distributed over many MOs (see Ref. 37 for detailed discussion of this phenomenon). Thus, in $Sc_3N@C_{78}$ ($D_{3h}$: 24109) and $M_3N@C_{92}$ ($D_3$: 85) the metal-cage interactions are better described by a "classical" covalent bonding while in majority of other clusterfullerenes the "back donation" scheme has to be applied as proposed by Liu et al.[37]

Based on Fig. 9, it can be concluded that the optimal Sc–N and Sc–C distances in $Sc_3N@C_{2n}$ are ca 2.05 and 2.30–2.35 Å, respectively. For small cage sizes, these parameters cannot be realized because there is not enough space for the cluster, and hence the cluster is strained by the carbon cage. The optimum geometry for $Sc_3N$ is realized in $Sc_3N@C_{80}$, and this is one of the reasons, besides stability of the cage alone, of the high yield of $Sc_3N@C_{80}$. For $Sc_3N@C_{80}$ the optimum distances are reached if the cluster resides in the center of the cage, while for larger cages the $Sc_3N$ cluster has to be displaced to one of the cage sides to preserve the optimum Sc–N and Sc–C bondlengths (Fig. 3). Apparently, displacement of the cluster from the cage center results in a less effective cluster-cage interaction as was already discussed above, and the $Sc_3N@C_{2n}$ clusterfullerenes with the cage size of $C_{82}$ and larger are not formed in detectable amounts. For $Y_3N@C_{2n}$, the optimum Y–N and Y–C distances may be

estimated as 2.25 and 2.50–2.55 Å, respectively. These values are reached for the cage sizes of $C_{90}$–$C_{98}$, and $Dy_3N@C_{2n}$ clusterfullerenes up to these cage sizes are observed.[21] In the larger cages displacement of the $M_3N$ cluster from the cage center can be expected, and it is one of the reasons why nitride clusterfullerenes with larger cage sizes are not formed.

**Conclusions**

Systematic quantum-chemical calculations of the hexaanions of empty fullerene cages, $C_{2n}^{6-}$, within a broad isomeric and compositional range ($2n$ = 68 – 98, more than 16000 isomers were considered for some of the compositions), followed by calculations of the $M_3N@C_{2n}$ (M = Sc, Y) clusterfullerenes based on the most stable cages resulted in the finding of the most stable $M_3N@C_{2n}$ isomers for the broad range of fullerene cage sizes. We have found that the most stable isomers always correspond to the structurally characterized clusterfullerenes, which enabled us to predict the cage structures for some $M_3N@C_{2n}$ compounds, whose structures are not yet experimentally described. The relative stability of the clusterfullerene isomers was found to be a function of both the relative stability of the 6-fold charged cage isomers and of the cage size and dimensional parameters. Moreover, the overall yield of the clusterfullerenes was shown to correlate well with the cage stabilities considered on the per-atomic basis, and the exceptional stability of $C_{80}^{6-}$ ($I_h$: 31924) and $C_{80}^{6-}$ ($D_{5h}$: 31923) fullerenes was found to be the reason for the high yield of the clusterfullerenes based on these cages, in spite of the unfavorable encapsulation energy for larger clusters. Moreover, the relative stability of the hexaanions of IPR isomers was found to correlate well with their hexagonal indices, while it is not generally true for uncharged fullerenes, and the exceptional stability of two most stable $C_{80}$ isomers was explained by the optimum distribution of pentagons on their surface minimizing the steric strain. In addition, the structures of the most stable non-IPR isomers of $C_{76}$ ($C_s$: 17490), $C_{78}$ ($C_2$: 22010), $C_{82}$ ($C_{2v}$: 39705) and $C_{84}$ (Cs: 51365) were found to be closely related to the $C_{80}$ ($I_h$: 31924) cage, which explains why these particular non-IPR isomers have the lowest energy. The binding energy of the cluster is analyzed as the function of the cage size, and it is found that for large cages the factors related to the cage size and

geometry become relatively unimportant. Finally, the study of the evolution of the cluster size and the metal-carbon distances with the increase of the cage size show that the optimum Sc–N and Sc–C distances for the $Sc_3N@C_{2n}$ family are reached at $2n = 80$, and further increase of the cage size is not favorable for the clusterfullerene formation. On the contrary, the optimum parameters for $Y_3N$ cluster are reached in $C_{90}$–$C_{98}$ cages, justifying the formation of larger cages than those in the $Sc_3N@C_{2n}$ family.

**Acknowledgment.** This work was supported by CRDF (A.A.P., award RUC2-2830-MO-06) and DAAD (A.A.P.). We thank Prof. Chun-Ru Wang (Institute of Chemistry, CAS, Beijing) for the program used to generate fullerene isomers, and Computing Center of Moscow State University for computer time.

**Supporting Information Available:** DFT-optimized Cartesian coordinates of the molecules listed in Tables 2–4, BE-1 and BE-2 values, and the figures showing structural relationships (i) between $C_{70}$ ($C_{2v}$: 8504), $C_{72}$ ($C_s$: 10528) and $C_{74}$ ($C_{2v}$: 14239) fullerenes and (ii) between $C_{82}$ ($C_s$: 39663) and $C_{78}$ ($D_{3h}$: 24109) and $C_{84}$ ($C_s$: 51365) fullerenes.

**References**

1. Akasaka, T.; Nagase, S., *Endofullerenes: A New Family of Carbon Clusters*. Kluwer Academic Publishers: Dordrecht, 2002.

2. Dunsch, L.; Yang, S. *Electrochem. Soc. Interface* **2006,** 15, (2), 34-39.

3. Dunsch, L.; Yang, S. *Small* **2007**, DOI: 10.1002/smll.200700036.

4. Stevenson, S.; Rice, G.; Glass, T.; Harich, K.; Cromer, F.; Jordan, M. R.; Craft, J.; Hadju, E.; Bible, R.; Olmstead, M. M.; Maitra, K.; Fisher, A. J.; Balch, A. L.; Dorn, H. C. *Nature* **1999,** *401*, 55-57.

5. Stevenson, S.; Fowler, P. W.; Heine, T.; Duchamp, J. C.; Rice, G.; Glass, T.; Harich, K.; E., H.; Bible, R.; Dorn, H. C. *Nature* **2000,** *408*, 427-428.

6. Olmstead, M. M.; Lee, H. M.; Duchamp, J. C.; Stevenson, S.; Marciu, D.; Dorn, H. C.; Balch, A. L. *Angew. Chem. Int. Ed.* **2003,** *42 (8)*, 900-903.

7. Olmstead, M. M.; de Bettencourt-Dias, A.; Duchamp, J. C.; Stevenson, S.; Marciu, D.; Dorn, H. C.; Balch, A. L. *Angew. Chem. Int. Ed.* **2001,** *40 (7)*, 1223-1225.

8. Duchamp, J. C.; Demortier, A.; Fletcher, K. R.; Dorn, D.; Iezzi, E. B.; Glass, T.; Dorn, H. C. *Chem. Phys. Lett.* **2003,** *375*, 655-659.

9. Krause, M.; Dunsch, L. *ChemPhysChem* **2004,** *5 (9)*, 1445-1449.

10. Cai, T.; Xu, L.; Anderson, M. R.; Ge, Z.; Zuo, T.; Wang, X.; Olmstead, M. M.; Balch, A. L.; Gibson, H. W.; Dorn, H. C. *J. Am. Chem. Soc.* **2006,** *128 (26)*, 8581-8589.

11. Yang, S.; Popov, A. A.; Dunsch, L. *Angew. Chem. Int. Ed.* **2007,** *46*, 1256-1259.

12. Dunsch, L.; Krause, M.; Noack, J.; Georgi, P. *J. Phys. Chem. Sol.* **2004,** *65*, 309-315.

13. Krause, M.; Wong, J.; Dunsch, L. *Chem. Eur. J.* **2005,** *11 (2)*, 706-711.

14. Iezzi, E. B.; Duchamp, J. C.; Fletcher, K. R.; Glass, T. E.; Dorn, H. C. *Nano Lett.* **2002,** *2 (11)*, 1187-1190.

15. Yang, S.; Dunsch, L. *Chem. Eur. J.* **2005,** *12 (2)*, 413-419.

16. Krause, M.; Dunsch, L. *Angew. Chem. Int. Ed.* **2005,** *44*, 1557-1560.

17. Stevenson, S.; Phillips, J. P.; Reid, J. E.; Olmstead, M. M.; P., R. S.; Balch, A. L. *Chem. Commun.* **2004**, 2814-2815.

18. Yang, S.; Kalbac, M.; Popov, A.; Dunsch, L. *ChemPhysChem* **2006,** *7 (9)*, 1990-1995.

19. Wang, X.; Zuo, T.; Olmstead, M. M.; Duchamp, J. C.; Glass, T. E.; Cromer, F.; Balch, A. L.; Dorn, H. C. *J. Am. Chem. Soc.* **2006,** *128*, 8884-8889.

20. Chen, N.; Zhang, E. Y.; Wang, C. R. *J. Phys. Chem. B* **2006,** *110 (27)*, 13322-13325.

21. Yang, S.; Dunsch, L. *J. Phys. Chem. B* **2005,** *109 (25)*, 12320-12328.

22. Beavers, C. M.; Zuo, T.; Duchamp, J. C.; Harich, K.; Dorn, H. C.; Olmstead, M. M.; Balch, A. L. *J. Am. Chem. Soc.* **2006,** *128 (35)*, 11352-11353.

23. Zuo, T.; Beavers, C. M.; Duchamp, J. C.; Campbell, A.; Dorn, H. C.; Olmstead, M. M.; Balch, A. L. *J. Am. Chem. Soc.* **2007,** *129 (7)*, 2035-2043.

24. Stevenson, S.; Lee, H. M.; Olmstead, M. M.; Kozikowski, C.; Stevenson, P.; Balch, A. L. *Chem. Eur. J.* **2002,** *8 (19)*, 4528-4535.

25. Yang, S.; Troyanov, S. I.; Popov, A. A.; Krause, M.; Dunsch, L. *J. Am. Chem. Soc.* **2006,** *128 (51)*, 16733-16739.

26. Olmstead, M. M.; de Bettencourt-Dias, A.; Duchamp, J. C.; Stevenson, S.; Dorn, H. C.; Balch, A. L. *J. Am. Chem. Soc.* **2000,** *122 (49)*, 12220-12226.

27. Wakahara, T.; Nikawa, H.; Kikuchi, T.; Nakahodo, T.; Rahman, G. M. A.; Tsuchiya, T.; Maeda, Y.; Akasaka, T.; Yoza, K.; Horn, E.; Yamamoto, K.; Mizorogi, N.; Slanina, Z.; Nagase, S. *J. Am. Chem. Soc.* **2006,** *128 (44)*, 14228-14229.

28. Shi, Z.-Q.; Wu, X.; Wang, C.-R.; Lu, X.; Shinohara, H. *Angew. Chem. Int. Ed.* **2006,** *45*, 2107-2111.

29. Wang, C. R.; Kai, T.; Tomiyama, T.; Yoshida, T.; Kobayashi, Y.; Nishibori, E.; Takata, M.; Sakata, M.; Shinohara, H. *Nature* **2000,** *408 (6811)*, 426-427.

30. Kato, H.; Taninaka, A.; Sugai, T.; Shinohara, H. *J. Am. Chem. Soc.* **2003,** *125 (26)*, 7782-7783.

31. Kobayashi, K.; Nagase, S.; Akasaka, A. *Chem. Phys. Lett.* **1995,** *245 (2-3)*, 230-236.

32. Kobayashi, K.; Nagase, S. *Chem. Phys. Lett.* **1997,** *274 (1-3)*, 226-230.

33. Campanera, J. M.; Bo, C.; Olmstead, M. M.; Balch, A. L.; Poblet, J. M. *J. Phys. Chem. A* **2002,** *106 (51)*, 12356-12364.

34. Krause, M.; Popov, A.; Dunsch, L. *ChemPhysChem* **2006,** *7 (8)*, 1734-1740.

35. Yang, S.; Kalbac, M.; Popov, A.; Dunsch, L. *Chem. Eur. J.* **2006,** *12 (30)*, 7856-7863.

36. Krause, M.; Liu, X.; Wong, J.; Pichler, T.; Knupfer, M.; Dunsch, L. *J. Phys. Chem. A* **2005,** *109 (32)*, 7088-7093.

37. Liu, D.; Hagelberg, F.; Park, S. S. *Chem. Phys.* **2006,** *330 (3)*, 380-386.

38. Campanera, J. M.; Bo, C.; Poblet, J. M. *Angew. Chem. Int. Ed.* **2005,** *44 (44)*, 7230-7233.

39. Popov, A. A.; Krause, M.; Yang, S.; Wong, J.; Dunsch, L. *J. Phys. Chem. B* **2007,** *111 (13)*, 3363-3369.

40. Dewar, M. J. S.; Zoebisch, E. G.; Healy, E.; Stewart, J. P. *J. Am. Chem. Soc.* **1985,** *107 (13)*, 3902-3909.

41. Granovsky, A. A. *PC GAMESS version 7.0,* **2006.** *http://classic.chem.msu.su/gran/gamess/index.html*.

42. Perdew, J. P.; Burke, K.; Ernzerhof, M. *Phys. Rev. Lett.* **1996,** *77 (18)*, 3865-3868.

43. Laikov, D. N. *Chem. Phys. Lett.* **1997,** *281*, 151-156.

44. Laikov, D. N.; Ustynyuk, Y. A. *Russ. Chem. Bull., Int. Ed.* **2004,** *54 (3)*, 820-826.

45. Greenwood, N. N.; Earnshaw, A., *Chemistry of the Elements*. Pergamon: Oxford, U.K., 1984.

46. Fowler, P. W.; Manolopoulos, D. E., *An Atlas of Fullerenes*. Clarendon Press: Oxford, U.K., 1995.

47. Echegoyen, L.; Chancellor, J.; Cardona, C. M.; Elliott, B.; Rivera, J.; Olmstead, M. M.; Balch, A. L. *Chem. Commun.* **2006**, 2653-2655.

48. Slanina, Z.; Chen, Z.; Schleyer, P. v. R.; Uhlik, F.; Lu, X.; Nagase, S. *J. Phys. Chem. A* **2006,** *110 (6)*, 2231-2234.

49. Wang, C. R.; Georgi, P.; Dunsch, L.; Kai, T.; Tomiyama, T.; Shinohara, H. *Curr. Appl. Phys.* **2002,** *2 (2)*, 141-143.

50. Cao, B.; Wakahara, T.; Tsuchiya, T.; Kondo, M.; Maeda, Y.; AminurRahman, G. M.; Akasaka, T.; Kobayashi, K.; Nagase, S.; Yamamoto, K. *J. Am. Chem. Soc.* **2004,** *126 (30)*, 9164-9165.

51. Xie, S. Y.; Gao, F.; Lu, X.; Huang, R. B.; Wang, C. R.; Zhang, X.; Liu, M. L.; Deng, S. L.; Zheng, L. S. *Science* **2004,** *304 (5671)*, 699.

52. Wang, C. R.; Shi, Z. Q.; Wan, L. J.; Lu, X.; Dunsch, L.; Shu, C. Y.; Tang, Y. L.; Shinohara, H. *J. Am. Chem. Soc.* **2006,** *128 (20)*, 6605-6610.

53. Raghavachari, K. *Chem. Phys. Lett.* **1992,** *190 (5)*, 397-400.

54. Chen, Z.; Cioslowski, J.; Rao, N.; Moncrieff, D.; Buhl, M.; Hirsch, A.; Thiel, W. *Theor. Chem. Acc.* **2001,** *106*, 364-368.

55. Furche, F.; Ahlrichs, R. *J. Chem. Phys.* **2001,** *114 (23)*, 10362-10367.

56. Sun, G.; Kertesz, M. *J. Phys. Chem. A* **2001,** *105*, 5468-5472.

57. Sun, G. Y. *Chem. Phys. Lett.* **2003,** *367 (1-2)*, 26-33.

58. Park, S. S.; Liu, D.; Hagelberg, F. *J. Phys. Chem. A* **2005,** *109 (39)*, 8865-8873.

59. The basis set used in Ref. 33 comprised triple-ζ + polarization for C and N atoms and complex basis set for Sc (frozen core for 1s and 2sp shells, double-ζ for 3s and 3p electrons, triple-ζ for nd and (n+1)s electrons, and single Slater orbital for (n+1)p electrons).

60. Kobayashi, K.; Sano, Y.; Nagase, S. *J. Comput. Chem.* **2001,** *22 (13)*, 1353-1358.

61. We could not find the bonded state for $Sc_3N^{6+}$ and $Y_3N^{6+}$ clusters at the PBE/TZ2P level of theory, and hence point energies were used for $M_3N^{6+}$ calculated with the cluster geometries taken from $M_3N@C_{80}$ ($I_h$: 31924).

62. Classical Coulomb energy is determined as $q_1q_2 \cdot R^{-1}$, where $q_1$ and $q_2$ are charges of the particle and sphere, and $R$ is the radius of the sphere.

63. Gan, L.-H.; Yuan, R. *ChemPhysChem* **2006**, *7 (6)*, 1306-1310.

**TOC Figure**

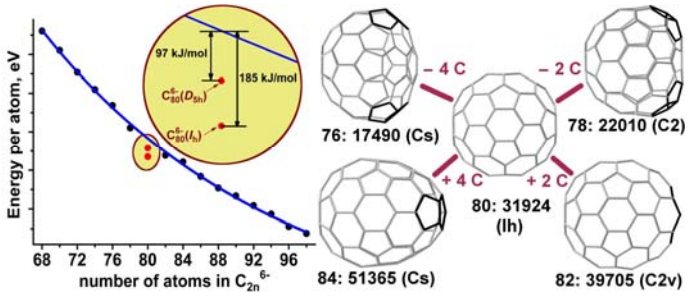
Energy per atom, eV
68 72 76 80 84 88 92 96
number of atoms in C2n6-
97 kJ/mol
185 kJ/mol
C80c6(D5h)
C80c6(Ih)
– 4 C
– 2 C
76: 17490 (Cs)
78: 22010 (C2)
+ 4 C
+ 2 C
80: 31924
(Ih)
84: 51365 (Cs)
82: 39705 (C2v)